

## ABSTRACT

Title of thesis: **CLOSED-LOOP FLUID RESUSCITATION: IN-SILICO STUDY**

Jonathan Cary Lucas V, Master of Science, 2015

Thesis directed by: **Dr. Jin-Oh Hahn**

**Department of Mechanical Engineering**

This thesis validates a control-oriented model of human circulatory dynamics associated with hemorrhage and fluid resuscitation, uses this model to design a series of closed-loop controllers for fluid resuscitation, and demonstrates the viability of these controllers by examining the performance of these controllers in an established model of human cardiovascular physiology. First, a recently developed control-oriented model of hemorrhage and fluid resuscitation was validated across diverse physiological conditions using an established model of human cardiovascular physiology, by employing a system identification procedure. Second, a series of closed-loop controllers were designed based on the nominal control-oriented model, including proportional control and proportional-derivative control based on the root locus analysis, as well as observer-based optimal state feedback control based on modern control theory. Third, the performance and robustness of the designed closed-loop controllers were validated using the established model of human cardiovascular physiology. The results suggested that model-based closed-loop control may be a viable alternative to today's manual fluid infusion practices.

# CLOSED-LOOP FLUID RESUSCIATION: IN-SILICO STUDY

by

Jonathan Lucas

Thesis submitted to the Faculty of the Graduate School of the  
University of Maryland, College Park in partial fulfillment  
of the requirements for the degree of  
Master of Science  
2015

Advisory Committee:

Associate Professor Jin-Oh Hahn, Chair/Advisor

Associate Professor Sarah Bergbreiter

Associate Professor Nikhil Chopra

© Copyright by  
Jonathan Cary Lucas V  
2015

## Acknowledgments

First, I have to acknowledge the main supporters of my pursuit of a master's degree: my family in their unwavering support and love, my girlfriend Rachel in her patience with the seemingly unending long hours and late nights, and my close friends for their help in the classroom and out.

Also, sincere thanks must go to my fellow researchers in the lab, particularly Ramin Bighamian and Xin Jin. Their constant evaluation of my work and their assistance in debugging the errors I experienced over the course of this year cannot be overstated. Not only is their hard work the basis for the research I did, but their continual support is what saw this project through to its conclusion. Their contributions were invaluable and this would not have been possible without their support.

Next, I must acknowledge my adviser Dr. Hahn for accepting me into his research group, even with a short time frame and restrictions on my coursework and schedule. I knew that supporting me in this thesis meant extra work for him and I sincerely appreciate his attention and dedication in helping me complete this thesis. His guidance is the primary reason this work exists. My only hope is that the research I have completed over this year can contribute in some small way to the great work his lab is doing. It has been a once in a lifetime opportunity, and Dr. Hahn's support is what made it such a meaningful experience.

Also, sincere thanks must be extended to my thesis committee, Professor Bergbreiter and Professor Chopra, for taking time out of their busy schedules to analyze and respond to my work. Their efforts were essential to this finished product and helped shape it product into a meaningful research contribution.

Finally, I must thank my professors from the United States Naval Academy who had a great impact on my collegiate career and for accommodating my unusual schedule and educational aspirations: particularly, Professor Edwin Zivi, my capstone advisor, Professor Brad Bishop, who helped me to truly appreciate the diversity control system design enables, and CAPT Owen Thorp, USN for his mentorship and guidance throughout my time at USNA.

Thank you to you all.

## Table of Contents

|  |    |
|--|----|
| List of Figures  | v  |
| 1 – Introduction                                       | 1  |
| 1.1 – Background and Significance                      | 1  |
| 1.2 – State-of-the-Art and Challenges                  | 2  |
| 1.3 – Thesis Goal                                      | 3  |
| 2 – System Identification of Blood Volume Dynamics     | 4  |
| 2.1 – Model  | 4  |
| 2.2 – System Identification                            | 6  |
| 2.2.1 – Guyton’s Model                                 | 6  |
| 2.2.2 – Randomized Data                                | 7  |
| 2.2.3 – Model Identification                           | 13 |
| 2.2.4 – Results and Discussion                         | 15 |
| 3 – Model-Based Control of Fluid Resuscitation         | 20 |
| 3.1 – Proportional and Proportional-Derivative Control | 20 |
| 3.2 – Observer-Based State Feedback Control            | 33 |
| 3.2.1 – Linear Quadratic Regulator Design              | 36 |
| 3.2.2 – State Observer Design                          | 36 |
| 3.3 – Results and Discussion                           | 37 |
| 4 – Conclusions and Future Work                        | 48 |
| 4.1 – Conclusions                                      | 48 |
| 4.2 – Future Work                                      | 48 |
| Bibliography   | 50 |

# List of Figures and Tables

## Chapter 1

Table 1.1 – Comparison of Sources about Blood Volume Models

## Chapter 2

Table 2.1 – Patient Randomization Parameters

Table 2.2 – Resultant Guyton Variation

Table 2.3 – Variation in Optimized Parameters

Figure 2.1 – Low-Order Model of Human Cardiovascular System, Block Diagram

Figure 2.2 – Guyton’s Reduced Model, from Guyton’s Circulatory Physiology

Figure 2.3 – Blood Volume Plant Representation used in Optimization

Figure 2.4 – Result of Optimized Infusion Values, Compared to Guyton Data

Figure 2.5 – Root Locus of Nominal Third Order Blood Volume Transfer Function

Figure 2.6 – Root Locus of Nominal Transfer Function, Zoomed in on First Pole/Zero

## Chapter 3

Figure 3.1 – 100 Patient Bode Diagram - Check for Stability

Figure 3.2 – General Root Locus of Third Order Blood Volume Transfer Function

Figure 3.3 – Root Locus Diagram for PD Controller Design,  $z = -3.68e-6$

Figure 3.4 – Step Response, PD Controller Design,  $z = -3.68e-6$

Figure 3.5 – Root Locus Diagram for PD Controller Design,  $z = -7.845e-6$

Figure 3.6 – Step Response, PD Controller Design,  $z = -7.845e-6$

Figure 3.7 – Root Locus Diagram for PD Controller Design,  $z = -0.002$

Figure 3.8 – Step Response, PD Controller Design,  $z = -0.002$

Figure 3.9 – Root Locus Diagram for PD Controller Design,  $z = -0.009$

Figure 3.10 – Step Response, PD Controller Design,  $z = -0.009$

Figure 3.11 – Root Locus Diagram for PD Controller Design,  $z = -0.035$

Figure 3.12 – Step Response, PD Controller Design,  $z = -0.035$

Figure 3.13 – Root Locus Diagram for PD Controller Design,  $z = -1$

Figure 3.14 – Step Response, PD Controller Design,  $z = -1$

Figure 3.15 – Comparison of Various P, and PD Controller Values

Figure 3.16 – State Observer Feedback Model

Figure 3.17 – 100 Transfer Functions, P Control  
Figure 3.18 – Total Blood Volume, 100 Patients Simulated in Guyton’s Model, P Control  
Figure 3.19 – Blood Volume Dilution, 100 Patients Simulated in Guyton’s Model, P Control  
Figure 3.20 – 100 Patients Guyton Calculated Error, PD Control  
Figure 3.21 – 100 Transfer Functions, PD Control  
Figure 3.22 – Total Blood Volume, 100 Patients Simulated in Guyton’s Model, PD Control  
Figure 3.23 – Blood Volume Dilution, 100 Patients Simulated in Guyton’s Model, PD Control  
Figure 3.24 – 100 Patients Guyton Calculated Error, PD Control  
Figure 3.25 – 100 Transfer Functions, State Space Control  
Figure 3.26 – Total Blood Volume, 100 Patients Simulated in Guyton’s Model, State Space  
Control  
Figure 3.27 – Blood Volume Dilution, 100 Patients Simulated in Guyton’s Model, State Space  
Control  
Figure 3.28 – 100 Patients Guyton Calculated Error, State Space Control

# Chapter 1: Introduction

## 1.1: Background and Significance

There are currently no model-based closed-loop fluid resuscitation controllers. This is an important issue to address because human judgement of fluid resuscitation has been shown to be imprecise. Medical professionals are known to occasionally give incorrect fluid infusion to the patients they have been charged with in emergency medical situations. In a study of ambulance transports to a Houston hospital, researchers found that many patients were dying as a result of the infusion procedure in transit to the hospital [1]. The blame does not lie with these professionals: it is hard to give a proper fluid infusion because the blood volume state at the conclusion of an undetermined volume of hemorrhage is impossible to know. It is at best an educated guess at how much blood the patient has lost, or on how the blood volume relates to blood pressure, or how much fluid would be required to bring them back to the initial blood volume state.

This is where closed-loop fluid resuscitation becomes a critically important development. Measuring the blood volume dilution, then applying fluid through a control system removes the guesswork typically associated with fluid infusion. This technological development could revolutionize fluid infusion and potentially save lives. In particularly tense or dangerous situations (such as wide spread emergency care or military operation) it removes the split-second decisions and unintentionally high risk infusion procedures, supplanting them with a simple, cheap, yet effective control mechanism.

Closed-loop fluid resuscitation is a way to prevent avoidable deaths for patients under emergency medical care. Potentially, it could be implemented in a user friendly device such that effective fluid infusion could be started by a layperson before professional emergency medical

personnel even arrived. The lifesaving benefits of effective fluid infusion are well documented, and it logically follows that improving this process is worth pursuit. This work suggests an alternative to the current methodology of educated guesswork. If executed correctly, this technology could save lives.

## 1.2: State-of-the-Art and Challenges

No technology exists that combines measuring the current state of patient blood volume dilution with closed-loop control. The important enabling technology is the ability to measure blood volume dilution in a live patient in real time. Traditionally, the major measured state used by medical personnel is blood pressure. However, due to the many variables that biomechanically alter blood pressure outside of strictly the amount of blood lost, this is not necessarily a reliable state upon which to build a control system. The controllers in this thesis are designed around the ability to measure blood volume dilution, which is a new development in the field [2]. This advance allows a much more effective control system to be designed that will be effective throughout different stages of the infusion process.

In order for model-based control to be possible, a model of the human cardiovascular system must exist. As shown below in Table 1.1, a pre-existing complete model for fluid resuscitation does not exist. The table highlights how sparse the information on a closed-loop controller to model the human cardiovascular system and resuscitation is. This is where the group in Dr. Hahn's lab has contributed to the field: a comprehensive simplified model of the resuscitation system. This model is the basis of the controller design described in this thesis.

| Year | Author    | Application   | Plasma | RBC | ISF | BV-ISF | ECF-ICF | BP              |
|------|-----------|---------------|--------|-----|-----|--------|---------|-----------------|
| 1974 | Cervera   | Hemorrhage    | ×      | o   | ×   | Δ      | ×       | ×               |
| 1975 | Champion  | Hem & Resus   | o      | ×   | ×   | ×      | ×       | Linear in BV    |
| 1986 | Lewis     | Hem & Resus   | o      | o   | ×   | Δ      | ×       | Nonlinear in BV |
| 1990 | Wears     | Hem & Resus   | o      | o   | ×   | Δ      | ×       | Nonlinear in BV |
| 1995 | Mardel    | Hemorrhage    | o      | o   | ×   | Δ      | ×       | Nonlinear in BV |
| 1996 | Simpson   | Hem & Resus   | o      | o   | ×   | o      | ×       | Nonlinear in BV |
| 2006 | Hirshberg | Hem & Resus   | o      | o   | o   | Δ      | ×       | Nonlinear in BV |
| 1975 | Pirkle    | Resuscitation | o      | o   | o   | Δ      | Δ       | Function of BV  |
| 1988 | Hedlund   | Resuscitation | o      | ×   | o   | Δ      | o       | CVS Model       |
| 1988 | Mazzoni   | Hem & Resus   | o      | o   | o   | o      | o       | ×               |
| 1993 | Barnea    | Resuscitation | o      | o   | o   | o      | ×       | CVS Model       |
| 1996 | Carlson   | Resuscitation | o      | o   | o   | Δ      | o       | ×               |
| 2003 | Gyenge    | Hemorrhage    | o      | ×   | o   | o      | o       | ×               |
| 1997 | Svensén   | Resuscitation | o      | o   | o   | o      | ×       | ×               |
| 1999 | Drobin    | Resuscitation | o      | o   | o   | o      | ×       | Function of BV  |
| 2002 | Drobin    | Resuscitation | o      | o   | o   | o      | o       | Function of BV  |

*Table 1.1 – This table shows the missing information involved in modeling the human cardiovascular system. ‘o’ represents clear existence of the information in a given, paper, ‘x’ represents no information in the paper, and the ‘Δ’ represents some unclear information. In order: [3] [4] [5] [6] [7] [8] [9] [10] [11] [12] [13] [14] [15] [16] [17] [18].*

### 1.3: Thesis Goal

The goal of this thesis is to show the viability of model-based closed-loop control of fluid resuscitation. This required the validation of a recently developed control-oriented model of hemorrhage and fluid resuscitation, the creation of a randomized data bank of in-silico patients which represent diverse biophysical constitutions, and the creation of a fluid infusion controller robust enough to handle these diverse physiological constitutions. The final result will be a preliminary study of model-based closed-loop fluid resuscitation. On a larger scope, the goal is to take a significant step toward an improved method of fluid infusion.

## Chapter 2: System Identification of Blood Volume Dynamics

### 2.1: Model

In order to create a fluid infusion controller, a simple model of the human cardiovascular system was required. This research focused on the validation and utilization of a recently developed control-oriented model of blood volume response to hemorrhage and fluid infusion [19]. The block diagram of the model is shown below as Figure 2.1.

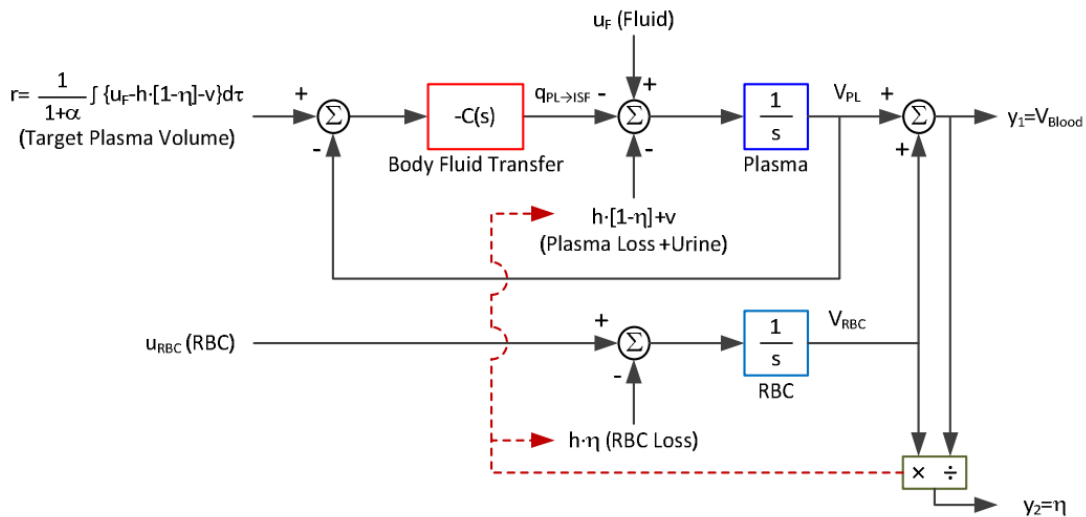


Figure 2.1 – A control-oriented blood volume model [19].

This model was designed to be physiologically transparent, as well as simple. It uses four variables to model a patient's blood volume response to both hemorrhage and infusion. The reference,  $r$ , in the above diagram is representative of target split of fluid in between the blood volume and the interstitial fluid volume. As is seen in the equation on the diagram, this is governed by the value of  $\alpha$ .

In the diagram,  $u_f$  represents the rate fluid infusion,  $h \cdot [1 - \eta]$  represents the rate of lost fluid from hemorrhage, and  $v$  represents the rate of urine. For this research, loss of fluid from urine is assumed to be zero, which simplifies the analysis. The output of the controller  $C(s)$ , is the rate of fluid transfer from blood plasma to interstitial fluid volume: this is denoted by the variable  $q_{PL \rightarrow ISF}$ . With these variables defined, it is easy to understand that the volume of plasma,  $V_{plasma}$ , is governed by:

$$V_{plasma} = \int [u_f - q_{PL \rightarrow ISF} - h(1 - \eta)] dt \quad (1)$$

The reference value  $r$  above, is now more clearly understood as the target ratio of volume:

$$r = \frac{1}{1 + \alpha} \int [u_f - h(1 - \eta)] dt \quad (2)$$

Furthermore, the transfer function  $C(s)$ , which is representative of the fluid transfer in between blood volume and interstitial fluid volume, is of the first order. It takes the form of:

$$C(s) = \frac{k_p + k_i}{s} \quad (3)$$

This value, in combination with the above block diagram, shows:

$$q_{PL \rightarrow ISF} = \frac{k_p + k_i}{s} (r - V_{plasma}) \quad (4)$$

The simplification of the above block diagram, with a scaling factor of the inverse of the initial blood volume for physical relevance, results in the following third order model:

$$G(s) = \frac{1}{BV_0} \frac{s^2 + \frac{k_p}{1 + \alpha} s + \frac{k_i}{1 + \alpha}}{s^3 + k_p s^2 + k_i s} \quad (5)$$

This is the model that will be validated with a complex representation of human cardiovascular physiology and used as the basis of the control design for this thesis. A bank of randomized transfer functions will be developed for design and analysis with this model.

## 2.2: System Identification

The validation of the control-oriented blood volume model involved several steps. First, a comprehensive full-scale cardiovascular physiology model (called the “Guyton’s model”; see Section 2.2.1) was modified in order to be applicable to the validation of the control-oriented blood volume model. Second, a bank of random patient data was created and run through the Guyton’s model to compile each patient’s ‘true’ response. A large sample size of 100 patients was selected to challenge the control system and demonstrate its robustness. The data produced by the Guyton’s model using this bank of patient characteristics were then fitted to the control-oriented blood volume model to yield patient-specific model parameters.

### 2.2.1: Guyton’s Model

The complex model that was used as the standard of the true human cardiovascular response for this thesis work was not created specifically for this research. The mathematical model was created by Arthur C. Guyton, M.D. and detailed in his series of books entitled Circulatory Physiology. The specific model used was presented in the third book in the series, Circulatory Physiology III: Cardiac Output and its Regulation [20]. It is an attempt to reduce the complexities of the human cardiovascular response to a block diagram. The diagram is shown as Figure 2.2.

The Guyton model itself is separated into eight major blocks, each of which models a different component of the cardiovascular response. These eight blocks are circulatory dynamics, interstitial fluid, autoregulation, sympathetic stimulation, pressure positive feedback, function curve adaptation, kidney output, and angiotensin. Each of these has a specific function in representing a different part of the real human cardiovascular system. For the duration of this research, the kidney output (via urine) was not considered.

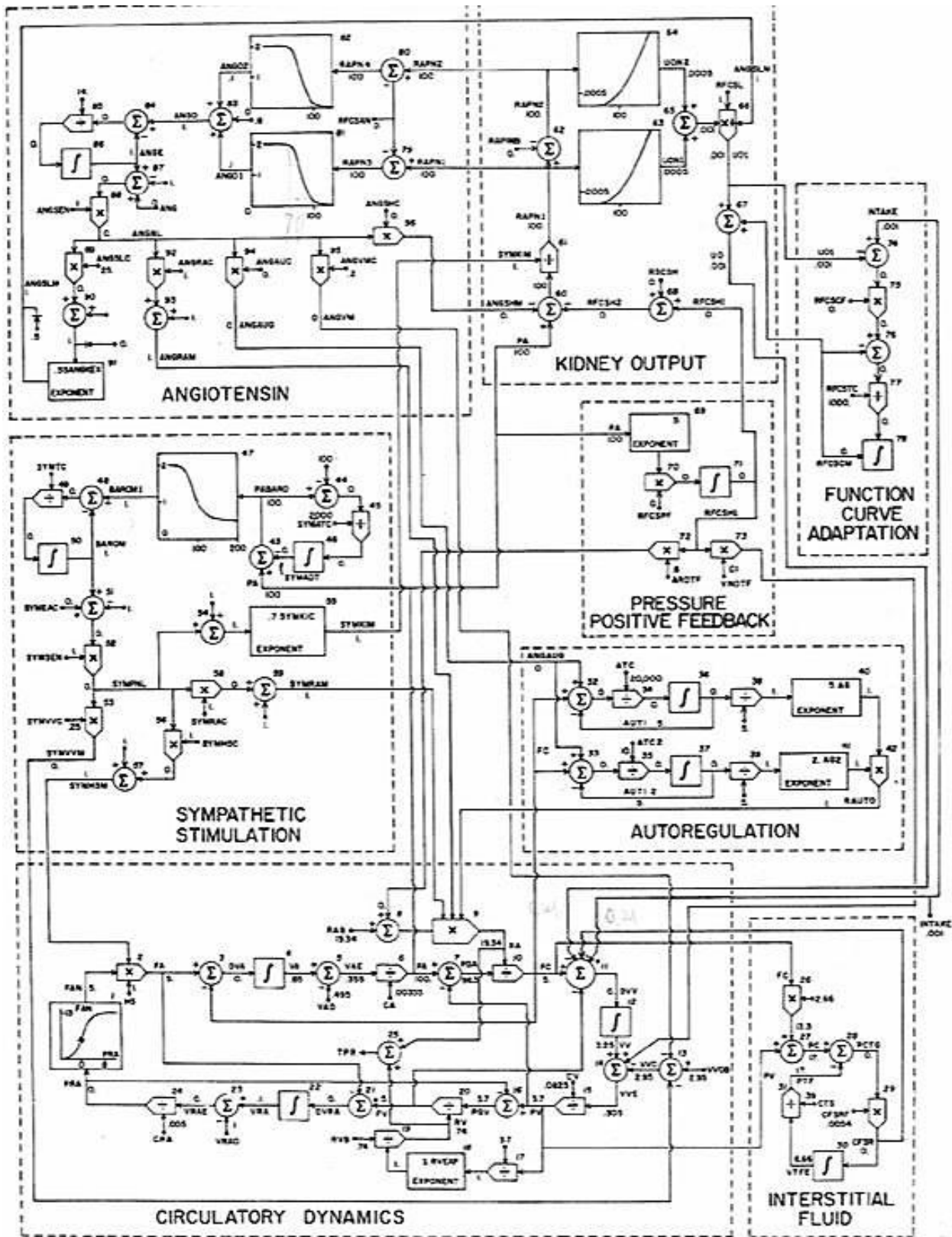


Figure 2.2 – This figure shows the reduced Guyton mode, as shown in the Guyton text [20].

In order to be employed for the validation of the control-oriented blood volume model, the Guyton's model required several changes. These were:

- A) Red Blood Cell Changes
- B) Total Volume
- C) Introduction of Hemorrhage and Infusion Functions
- D) Switch from a Variable-Step Solver to a Fixed-Step Solver

A) The model needed to be modified in order to consider the loss of red blood cell volume. As simple fluid hemorrhage and infusion occurred, the red blood cell volume, which constitutes about 40-45% of the total blood volume, will remain unchanged. This is an important consideration, as during the hemorrhage scenario, the red blood cell volume will be decreased, and the subsequent infusion will only use fluid to replace this volume.

B) Next, the total volume considered by Guyton's model had to be changed in order to be physically relevant. Initially, Guyton's model only considered three of the 5 major compartments of the human cardiovascular system. This means that the total blood volume considered was only around 3 liters. In order to bring this to a physically relevant value of around 5 liters, the original Guyton model was scaled appropriately using the nominal Guyton values. This simple change made the Guyton response easier to compare to the physical response.

C) The Guyton model did not explicitly contain any method of evaluating hemorrhage and infusion. Some level of analysis could be performed by manually altering the initial values in the Guyton model, but there was not a reproducible way of consistently modeling the same

hemorrhage for different patients using this method. The inclusion of hemorrhage and infusion functions allowed the introduction of realistic hemorrhage and infusion scenarios. By adding these functions to the model, the hemorrhage and infusion could be initiated at specific times in various scenarios, the amount removed or added could be specifically controlled, and the patients could have time to reach settled values before the scenario began. These functions were implemented in SIMULINK by adding step blocks that would apply a specific rate of hemorrhage and infusion to the venous system of Guyton's model at precisely controllable times.

D) In order to work with the hemorrhage and infusion scenarios, to enable direct comparison of the results with those of the control-oriented model, and to allow the translation of the results into the controller design space, the model had to be implemented with a fixed-step solver (ode3). The variable-step solver caused offset at the beginning of the hemorrhage and infusion scenarios from patient to patient and the different start and stop times made the control analysis impossible.

The major issue with Guyton's model, in terms of applying a fluid controller, is the complexity of the model. The scale and intricacy of Guyton's model were prohibitive. Running one patient through the model to evaluate the response to both hemorrhage and infusion took up to 15 minutes of computing time, and created variables with lengths up to 700,000 values. This is where the importance of a control-oriented model became most clear.

## 2.2.2: Randomized Patient Data

In order to validate the control-oriented blood volume model via system identification, a set of random patients was created using the Guyton's model. The goal was to create diverse patient models having a wide range of hemodynamic responses. For this purpose, a few key parameters in the Guyton's models were randomly perturbed. These parameters and their physical meanings are:

RAB – Basic arterial resistance

HS – Heart strength coefficient, which modifies the cardiac output

VVOB – Unstressed venous volume

SYMVVC – Coefficient in sympathetic system that models sympathetic effect on unstressed volume

SYMHSC – Sympathetic heart strength coefficient

SYMRAC – Sympathetic representation of arterial resistance

SYMKIC – Evaluates sympathetic effect on transfer to kidneys

ANGSLC – Modification of the slope of the renal curve by the angiotensin system

Each parameter was randomized using MATLAB's `rand` command. This pseudorandom number generator was used to create eight different weighting variables. Each weighting variable was added to the nominal Guyton value to produce a randomized value within  $\pm 20\%$  of the nominal value. This random generation of patient parameters was performed 100 times in order to create a bank of 100 randomized patients for use in Guyton simulation.

The difference between patient values was analyzed, and deemed to be sufficient by looking at the standard deviation, mean, minimum, and maximum. These values, when run through Guyton's model, produced variation in initial blood volume as much as 1.5 Liters. Considering the nominal patient has a blood volume of about 5 liters, this is a significant difference. This range was important to show the robustness of the controllers in providing fluid

infusion. This bank of 100 patients was saved individually. This same data bank was used for all steps of the controller design and testing. Details on the variation in the randomized parameters are shown in Table 2.1 below.

| Parameter | Guyton Value | Mean    | Standard Deviation | Median  | Minimum | Maximum |
|-----------|--------------|---------|--------------------|---------|---------|---------|
| RAB       | 19.34        | 20.8333 | 5.6320             | 21.3237 | 10.3005 | 28.4873 |
| HS        | 1            | 0.9854  | 0.2853             | 1.0047  | 0.5012  | 1.4880  |
| VVOB      | 2.95         | 2.8115  | 0.8428             | 2.7191  | 1.4887  | 4.3621  |
| SYMVVC    | 25           | 26.3184 | 6.9708             | 26.1803 | 12.6679 | 37.4034 |
| SYMHSC    | 1            | 1.0527  | 0.2788             | 1.0472  | 0.5067  | 1.4961  |
| SYMRAC    | 1            | 1.0527  | 0.2788             | 1.0472  | 0.5067  | 1.4961  |
| SYMKIC    | 0.7          | 0.7369  | 0.1952             | 0.7330  | 0.3547  | 1.0473  |
| ANGSLC    | 25           | 24.6047 | 7.5887             | 25.0169 | 13.2635 | 37.4770 |

*Table 2.1 – This table shows the variation of the randomized parameters*

These randomized values were then run through Guyton’s model with a step hemorrhage and a step infusion of 2 liters respectively. The responses for all 100 patients were recorded and calculated. The variation in these parameters resulted in a wide range of patient responses which are detailed in Table 2.2 below:

|                         | Mean   | Standard Deviation | Max    | Min    |
|-------------------------|--------|--------------------|--------|--------|
| BV0 - Guyton            | 4.9748 | 0.2991             | 5.4938 | 4.3856 |
| BV0 – Infusion Guyton   | 4.3578 | 0.2452             | 4.8540 | 3.8521 |
| Alpha – Guyton          | 2.3198 | 0.5090             | 3.4344 | 1.3471 |
| Alpha – Infusion Guyton | 2.3365 | 0.5146             | 3.3256 | 1.3447 |

*Table 2.2 – This table shows the variation of the Guyton values based on the randomization*

BV0 above is a measure of the blood volume dilution at the beginning of the hemorrhage scenario (BV0 – Guyton) and then again at the beginning of the infusion scenario (BV0 – Infusion Guyton). Similarly, alpha is a calculation of the transfer between blood volume and interstitial fluid volume. These two values were the most important in terms of building a controller to control fluid infusion, and checking whether Guyton’s model had produced the correct response.

### 2.2.3: Model Identification

In order to introduce the 100 randomized patients of Guyton’s model to the recently developed blood volume model, the four characteristic variables (Alpha, Kp, Ki, and BV0) from each patient had to be determined. This was achieved primarily using the optimization function `fmincon` in MATLAB. This function used the real patient response to a step hemorrhage and infusion to create optimized values for the characteristic variables above. This function generally works by simultaneously minimizing a series of equations. In this case, the response of the

control-oriented model was compared to the results for the same infusion from the Guyton model. The initial guess was set at the values from the nominal case, and then the function was run. The function `fmincon` tried thousands of combinations of characteristic variables, until a set that minimized the error was found. The SIMULINK model that was used in tandem with `fmincon` to create the characteristic variables for all 100 is shown in the following Figure 2.3:

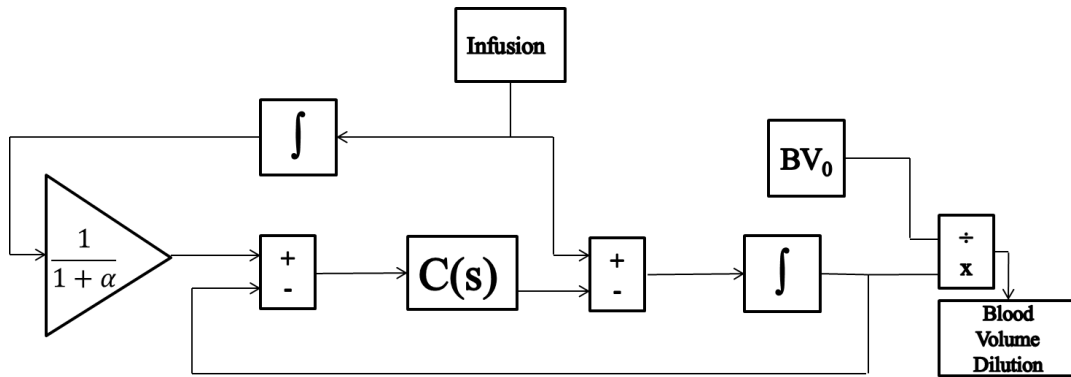


Figure 2.3 – This figure shows the control-oriented blood volume model, used by the optimization function to reduce 100 patients in Guyton’s model, into 100 sets of four characteristic variables.

The optimized values were then saved for each patient. The data from the 100 patient bank are represented in the following table, Table 2.3:

|                         | Mean      | Standard Deviation | Max       | Min        |
|-------------------------|-----------|--------------------|-----------|------------|
| Alpha                   | 1.8893    | 0.4196             | 2.7921    | 1.0689     |
| Alpha - Infusion        | 2.4405    | 0.4251             | 3.3256    | 1.5285     |
| BV0                     | 5.8131    | 0.3475             | 6.4749    | 5.1093     |
| BV0 – Infusion          | 4.1841    | 0.1855             | 4.6237    | 3.7705     |
| Ki                      | 2.920e-7  | 1.6762e-7          | 1.0059e-6 | 3.4729e-9  |
| Ki - Infusion           | 1.0840e-7 | 1.1491e-7          | 6.5315e-7 | 9.0405e-10 |
| Kp                      | 0.0307    | 0.0024             | 0.0365    | 0.0261     |
| Kp - Infusion           | 0.0167    | 0.0014             | 0.0196    | 0.0139     |
| Fitting error           | 0.0023    | 0.0233             | 0.2325    | 0          |
| Fitting error- Infusion | 0.0020    | 0.0205             | 0.2050    | 0          |

*Table 2.3 – This table shows the variation of the optimized controller values based on the randomized parameters*

With these results, and the equations shown above, 100 transfer functions representing 100 patients could be produced and used for further analysis. These patients showed a high degree of randomization, and were suitable for designing a controller.

#### 2.2.4: Results and Discussion

The results of the optimization were shown to be accurate by comparison to the real response. This is shown in Figure 2.4 below, for the nominal patient. For the nominal patient, the following values were found by the optimization function:

$$\begin{aligned} \alpha &= 2.285 \\ BV_0 &= 4.168 \\ K_p &= 0.017 \\ K_i &= 1.310e-7 \end{aligned}$$

Of particular note is the value of  $\alpha$ , the variable that primarily determines the ratio of fluid transfer from the blood volume to the interstitial fluid volume. According to Guyton's text, a value of 2.3 is expected. The results being so close to the expected value validated the optimization results and showed that the Guyton simulation, the optimization, and the reduced blood volume model had worked correctly.

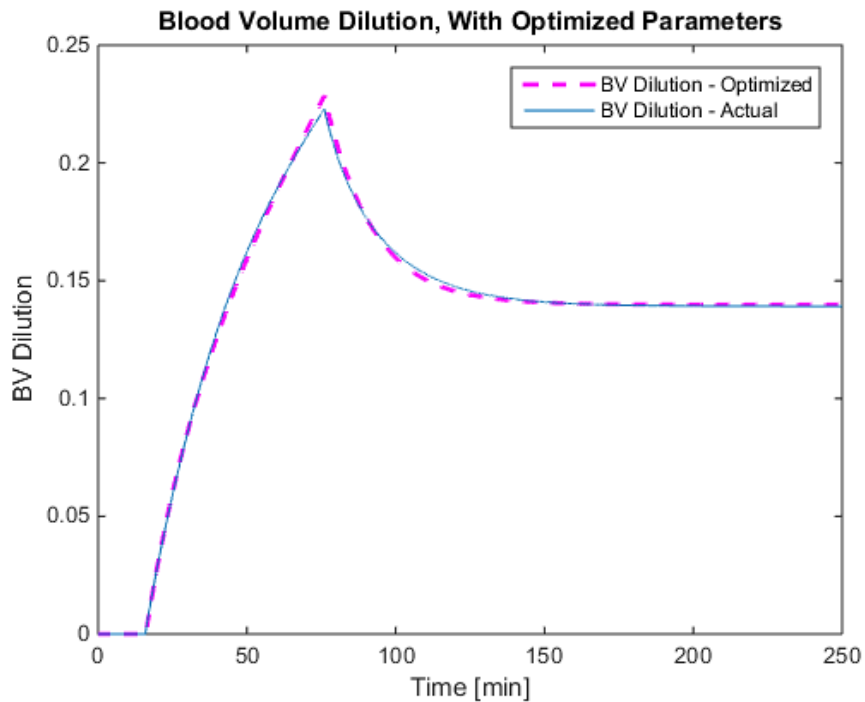


Figure 2.4 – This plot shows the optimized values for the infusion response, plotted against the actual infusion response of Guyton's model

These optimization values could then be used to create the traditional third order transfer function of the control-oriented blood volume model. This could also be rearranged to find its equivalent poles and zeros. Transfer functions were determined from the above equation and then expanded in the following manner:

$$G(s) = \frac{K * (s + z1) * (s + z2)}{s * (s + p1) * (s + p2)} \quad (6)$$

Again, for the case of the nominal patient, this resulted in the following values:

$$\begin{aligned} K &= 0.23993 \\ p1 &= 0.0167 \\ p2 &= 7.84e-6 \\ z1 &= 0.0049 \\ z2 &= 7.85e-6 \end{aligned}$$

These values were analyzed using root locus analysis, as shown below in Figure 2.5.

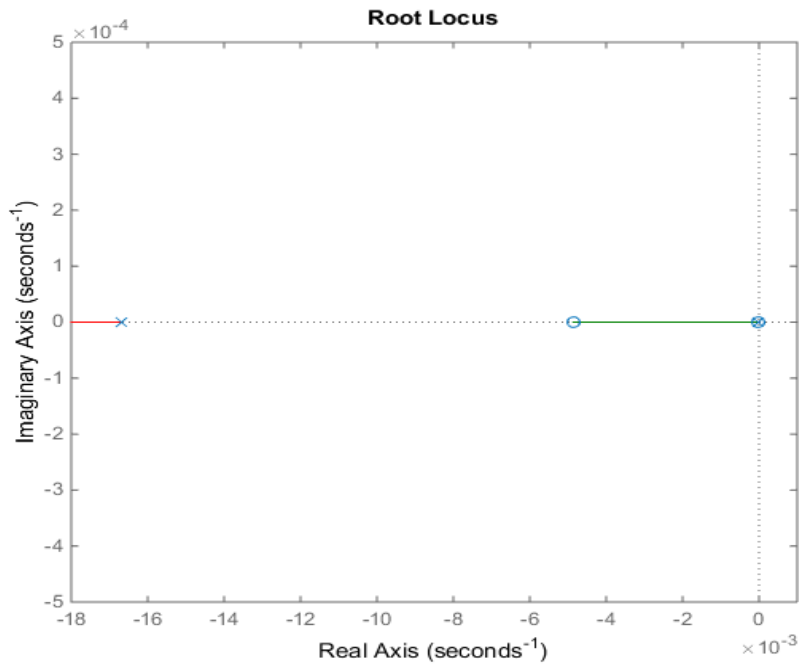


Figure 2.5 – This figure shows the general root locus for the third order model.

The most densely populated area of the root locus is only visible at a much higher level of zoom: that is the region where the first pole and zero interact. This high level of zoom is shown in Figure 2.6.

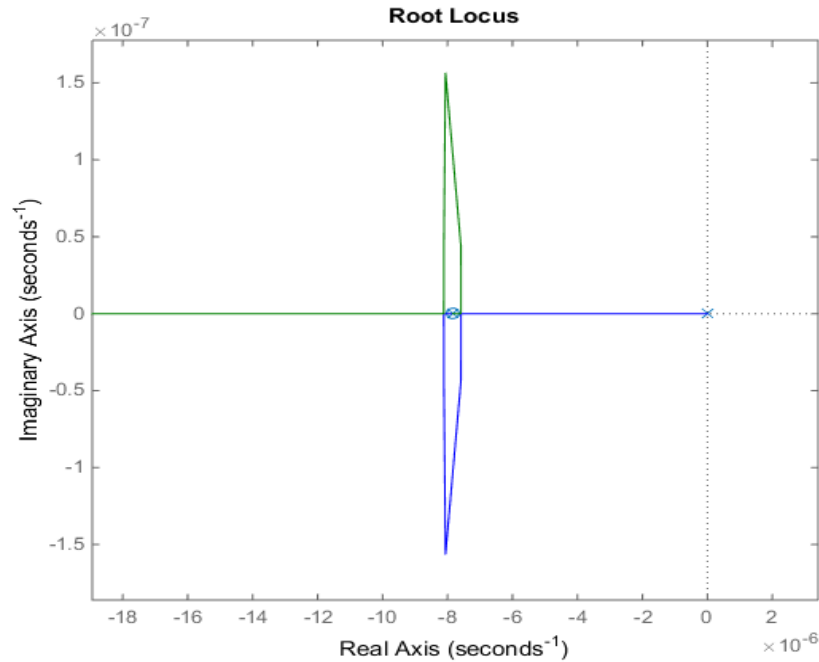


Figure 2.6 – This figure shows the interaction of the first pole and zero for the nominal patient.

In this chapter, the Guyton model was considered to be the standard patient response. With this assumption, a bank of randomized patients was created based on several key variables to modify Guyton’s model. This was an attempt to set up the design process for a controller that can handle a wide variety of patients. As demonstrated above, the randomization created a high degree of variability in the Guyton response. These randomized patients were then simulated, and their responses were fitted to the control-oriented model via the system identification.

It is noted that the dynamics of the infusion pump was not included in the model, which is a reasonable simplification because the dynamics of the patient response to fluid infusion is much slower than the dynamics of the infusion pump.

## Chapter 3: Model-based Control of Fluid Resuscitation

Last chapter, 100 randomized patients were analyzed using optimization in MATLAB to create 100 control-oriented blood volume models, representing each patient's dynamic input-output relationship between fluid infusion and blood volume response. The next step was to design a series of closed-loop controllers that will deliver an efficient infusion to a variety of patients, based on measured patient responses. First, the stability of the patient data bank was analyzed using a Bode plot. This was followed by designing a proportional (P) controller, a proportional-derivative (PD) controller, and state-feedback/observer-feedback controllers. These controllers were all designed for the nominal patient (associated with the nominal Guyton model) and then tested against all 100 randomized patient models. Once all 100 randomized patient models worked in simulation, the controller was then placed in the Guyton's model, to determine if it would provide the correct infusion for the complex model representing the real patient.

### 3.1: Proportional and Proportional-Derivative Control

The first step used in designing a controller was to look at the Bode diagrams for all 100 patients. The most efficient way to do this was to show all 100 patient Bode plots on top of one another as shown below in Figure 3.1.

As the Bode Diagram clearly shows, the phase diagram will never cross -180 degrees for any patient. This is significant as it shows that all 100 patient plants are stable at all frequencies. With the stability demonstrated, the next step was to implement proportional control.

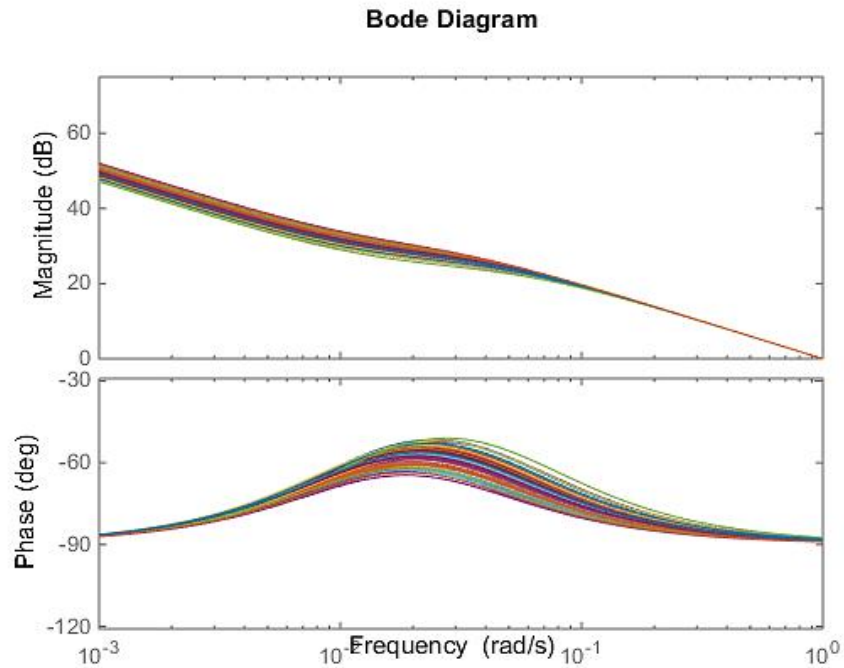


*Figure 3.1 – This Bode Diagram shows the stability of all 100 patients in simulation*

The plant is the base blood volume model as outlined above, with each patient's characteristic variables creating a different plant. For the design of the proportional controller, it is useful to look at the root locus of the transfer function of the nominal patient, shown below as Figure 3.2.

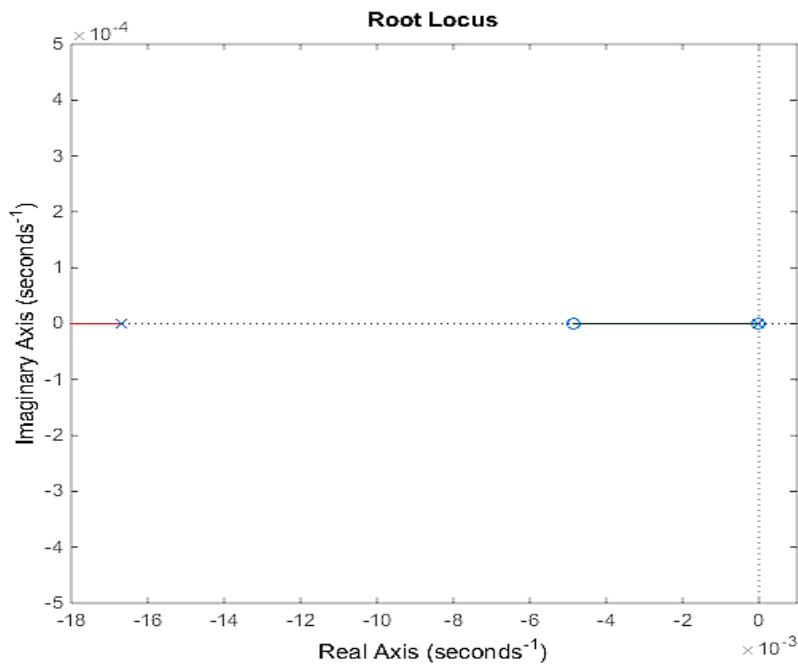


Figure 3.2 – This figure shows the general root locus for the third order model.

As shown by the above root locus, all the possible responses for different gain values lie to the left of the imaginary axis. This means that for all values of gain, the plant will be stable, and produce a response. The root locus shows that proportional control will work for all cases, and will work to move the pole on the imaginary axis to the zero that is furthest away. This will speed up the settling time of the system without significant impact on the steady state error.

In order to turn this open loop model into a proportional controller, feedback was added for blood volume dilution as well as a gain block. Also, saturation values were added in order to model the parameters of available real life infusion pumps. A saturation value characteristic of the parameters of real pumps was selected and set at 0.105 [L/min] [21]. The selection of this value was non-trivial, because under all simulated situations there was some level of control

saturation. The saturation minimum was set to zero, as removing infused fluids from a patient would be physically irrelevant. This saturation value was used for all the controller design.

As for the proportional derivative controller, the location of the zero was evaluated at each possible location in relation to the poles and zeros, and then the response to a step command set to 1, when  $t = 0$  was analyzed for comparisons sake. The responses are shown in the following root locus diagrams, and the resulting step response.

The response of the system with a zero at the first location,  $z = -3.68e-06$ , is shown as Figure 3.3 and its response to a step input is shown as Figure 3.4.

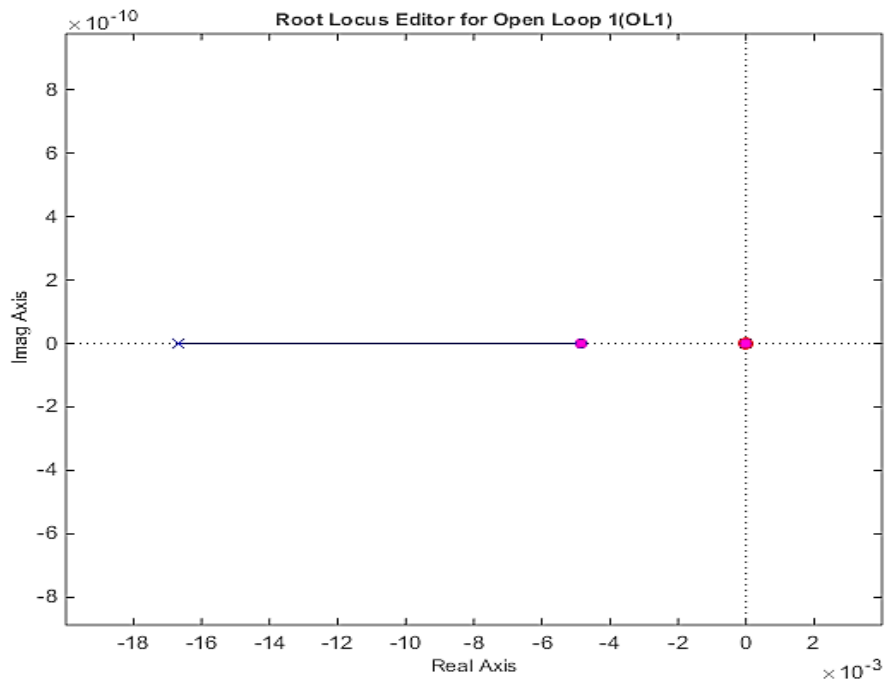
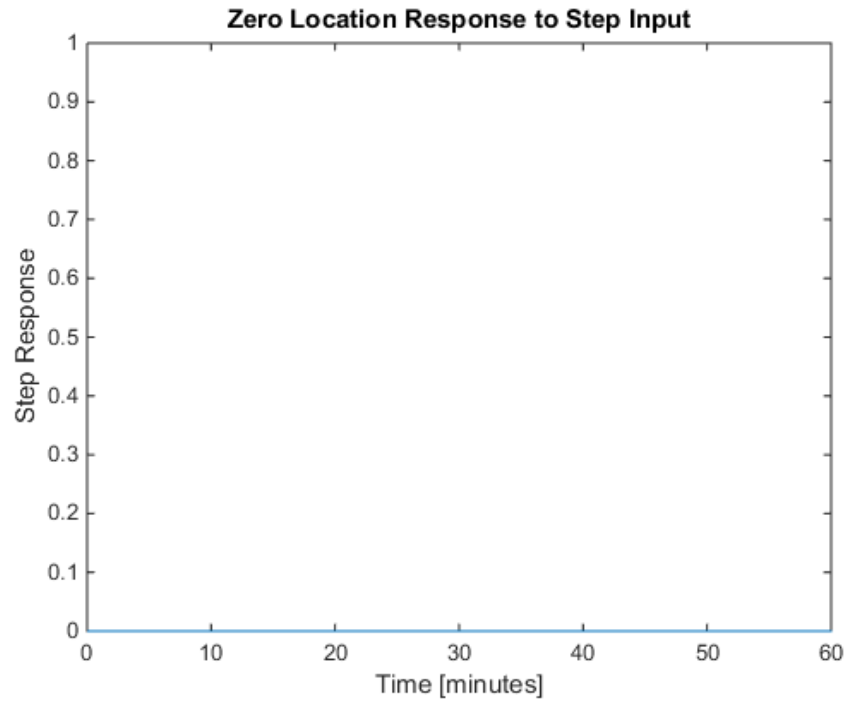


Figure 3.3 – This figure shows the root locus for a zero placed at the first location.



*Figure 3.4 – This figure shows the response of the step command for the proportional derivative controller above.*

The response of the system with a zero at the second location,  $z = -7.845e-6$ , is shown as Figure 3.5 and its response to a step input is shown as Figure 3.6.

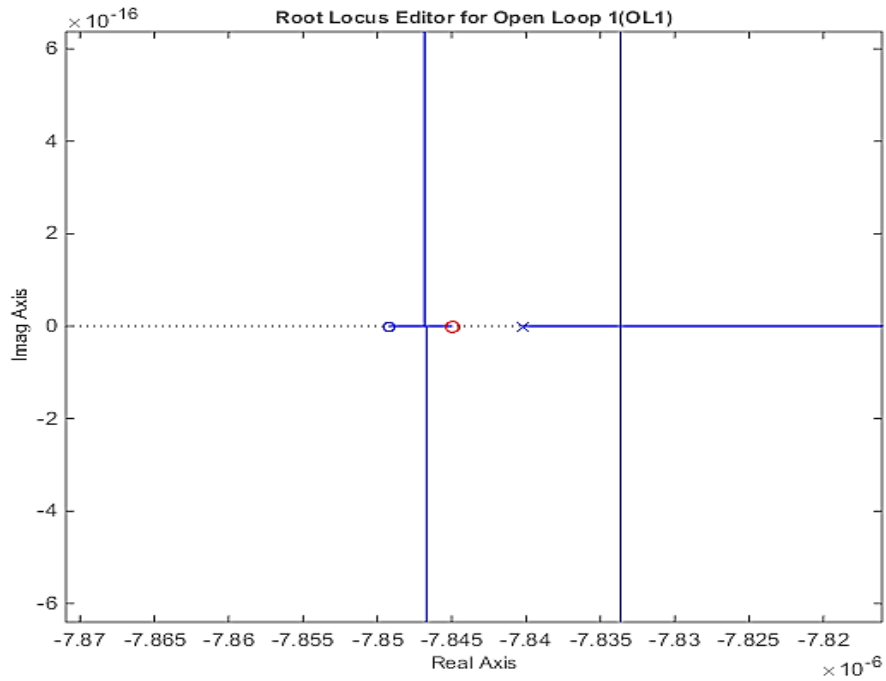


Figure 3.5 – This figure shows the root locus for a zero placed at the second location. It has been zoomed in to show the effect of this zero on its immediate neighbors. Red indicates the added zero.

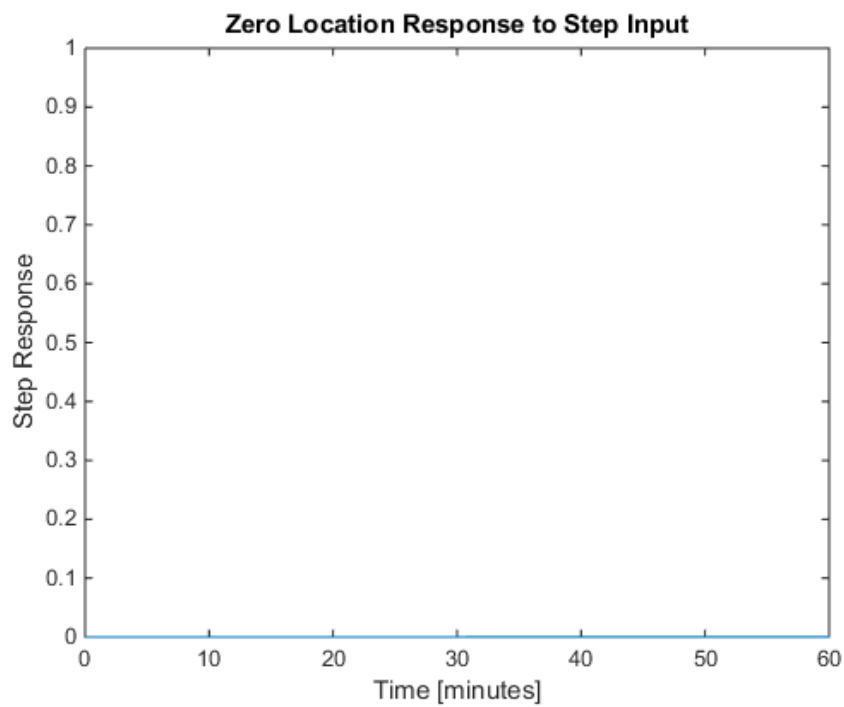


Figure 3.6 – This figure shows the response of the step command for the proportional derivative controller above.

The response of the system with a zero at the third location,  $z = -0.002$ , is shown as Figure 3.7 and its response to a step input is shown as Figure 3.8.

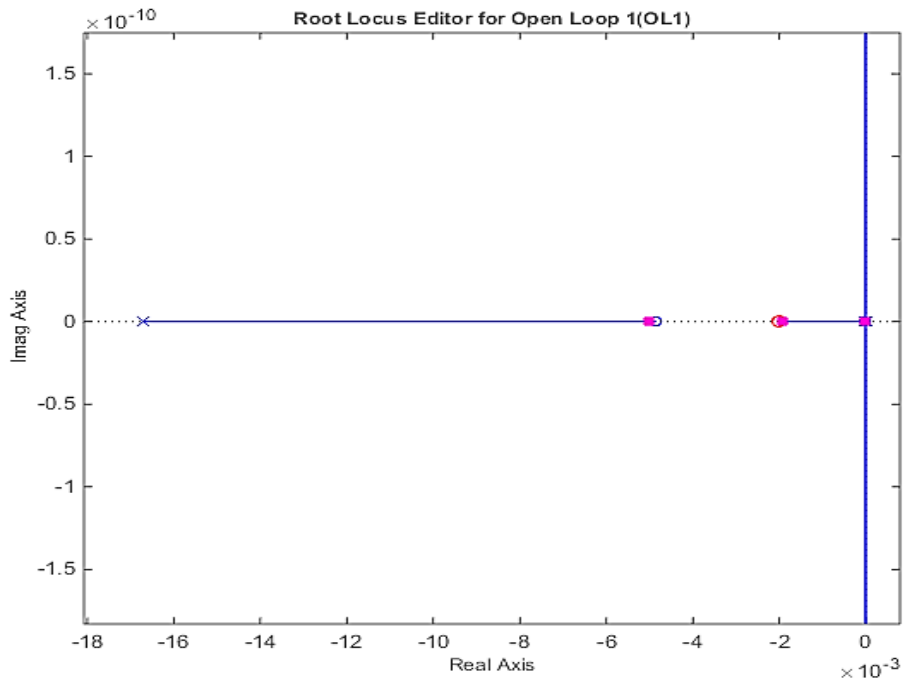
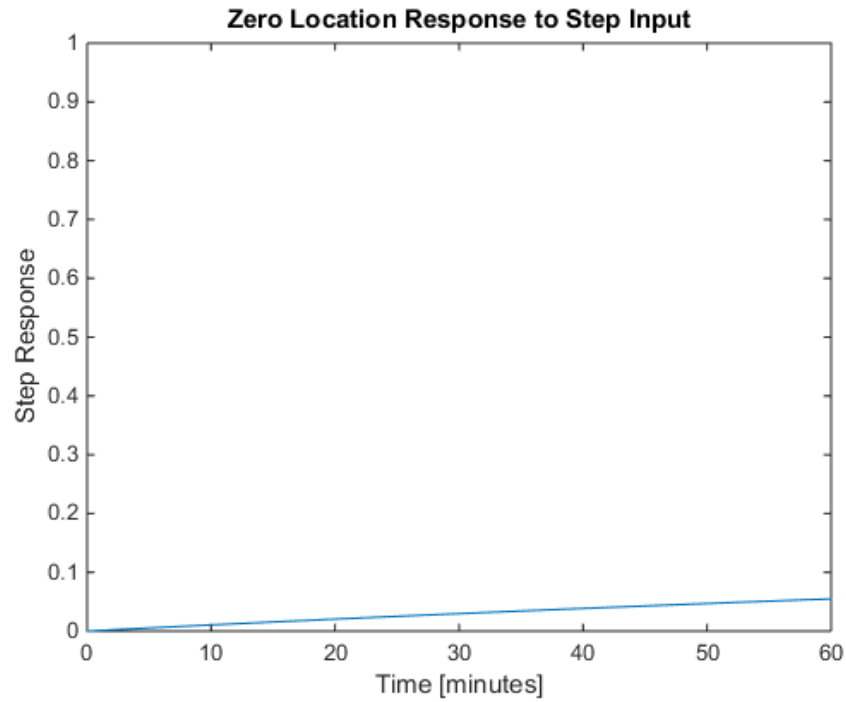


Figure 3.7 – This figure shows the root locus for a zero placed at the third location.



*Figure 3.8 – This figure shows the response of the step command for the proportional derivative controller above.*

The response of the system with a zero at the fourth location,  $z = -0.009$ , is shown as Figure 3.9 and its response to a step input is shown as Figure 3.10.

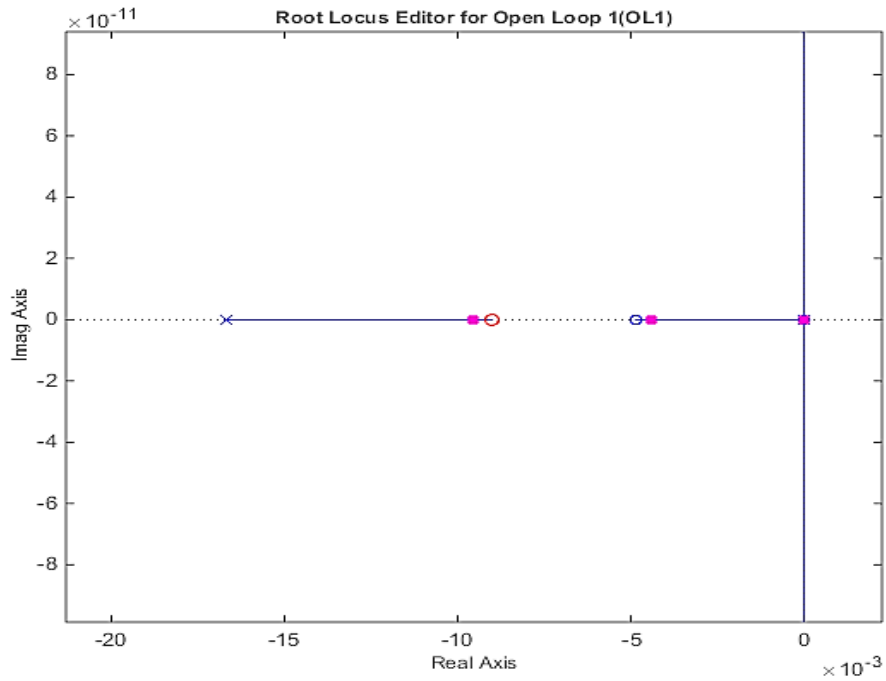


Figure 3.9 – This figure shows the root locus for a zero placed at the fourth location.

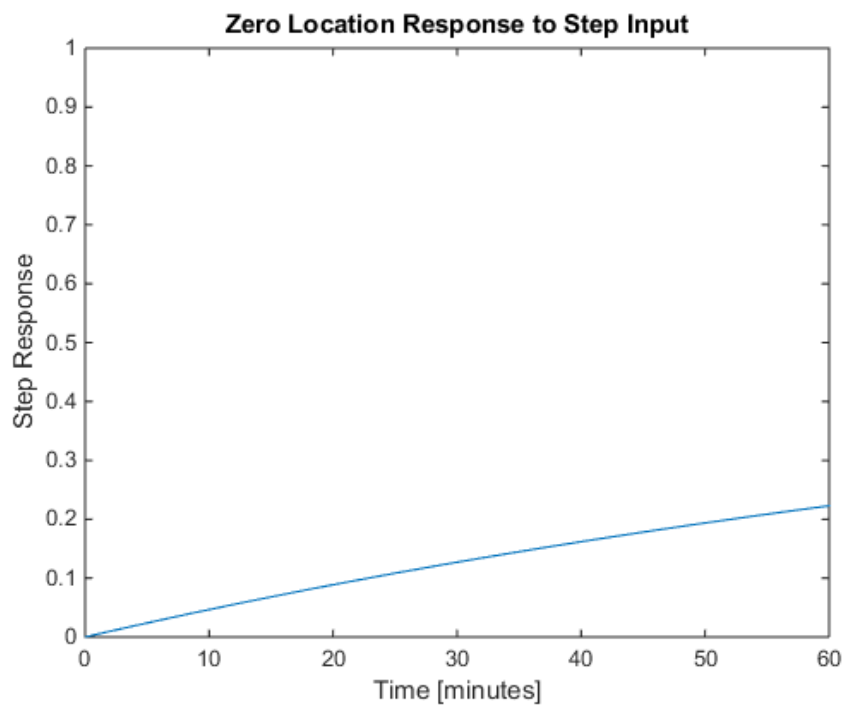
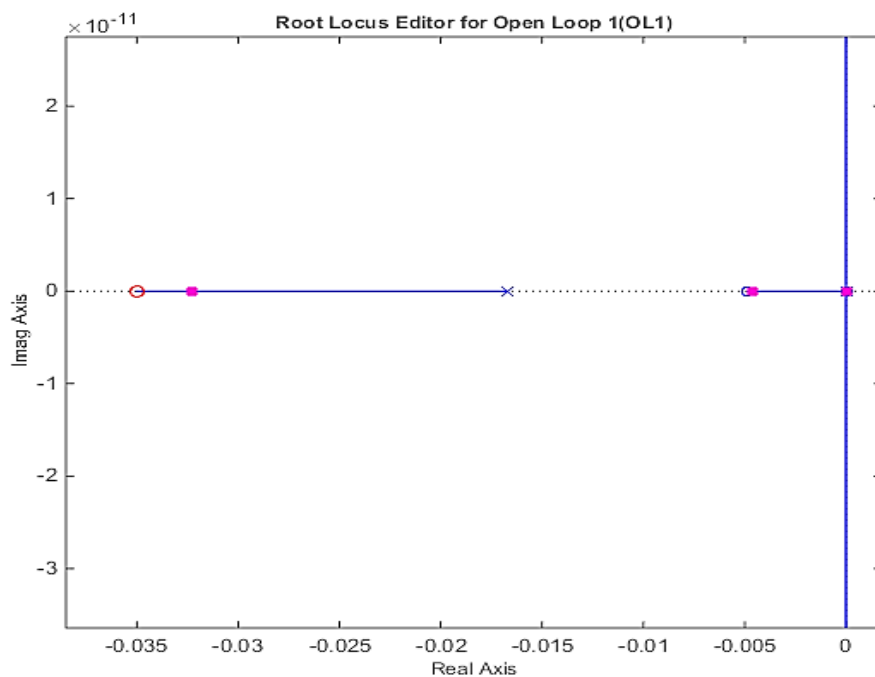


Figure 3.10 – This figure shows the response of the step command for the proportional derivative controller above.

The response of the system with a zero at the fifth location,  $z = -0.035$ , is shown as Figure 3.11 and its response to a step input is shown as Figure 3.12. Then the next figures show the root locus and step response to a zero location much further out on the real axis, with  $z = -1$ , as Figure 3.13 and Figure 3.14.



*Figure 3.11 – This figure shows the root locus for a zero placed at the fifth location.*

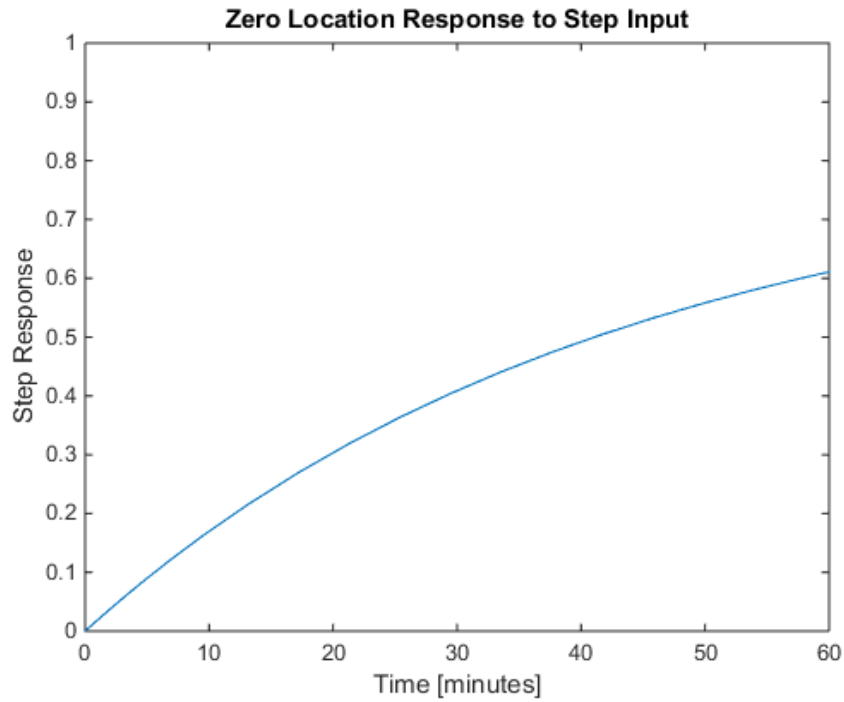


Figure 3.12 – This figure shows the response of the step command for the proportional derivative controller above.

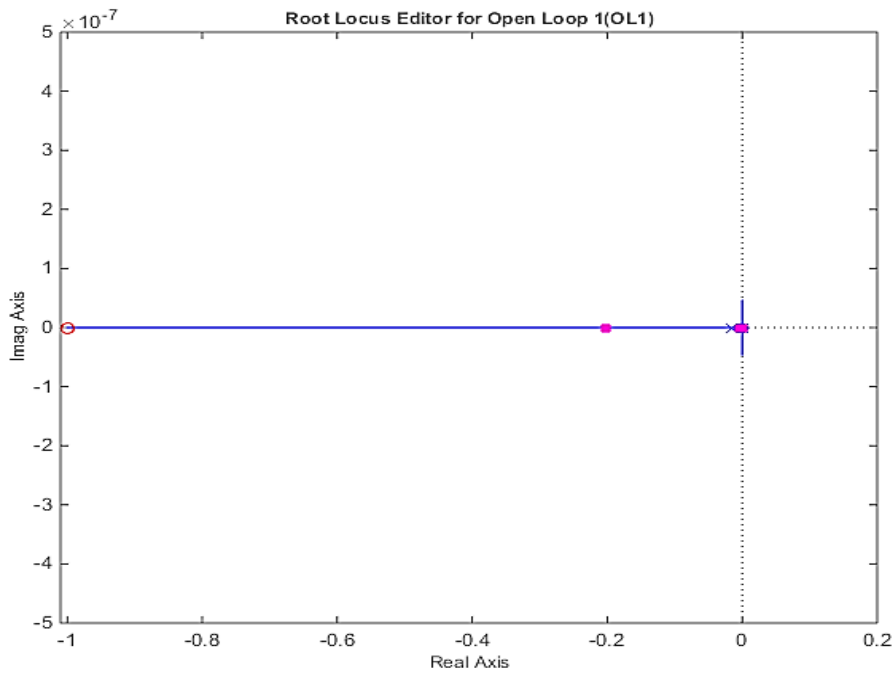
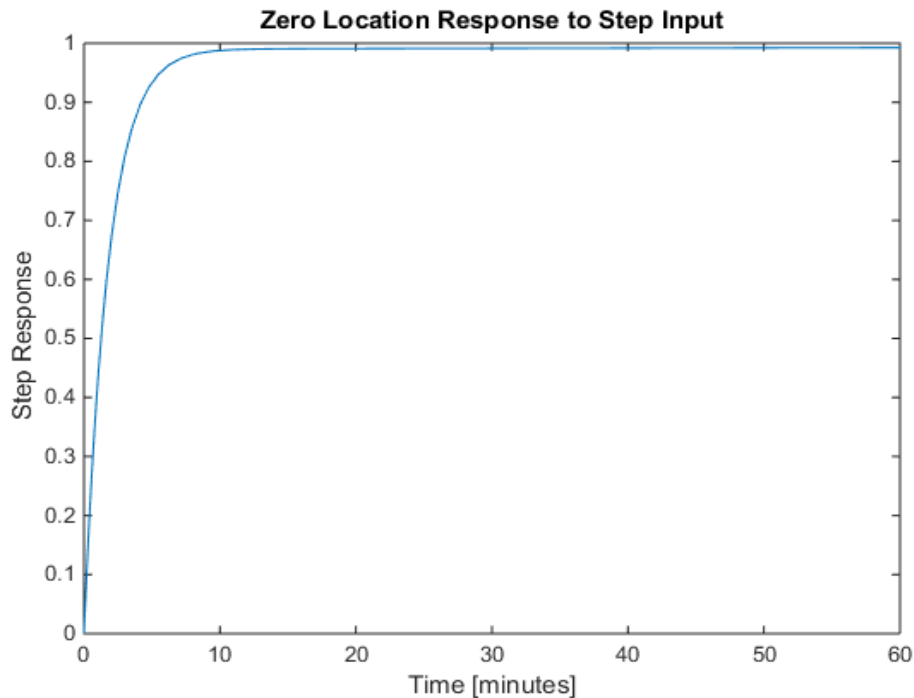


Figure 3.13 – This figure shows the root locus for a zero placed at the sixth location.



*Figure 3.14 – This figure shows the response of the step command for the proportional derivative controller above.*

As the above root loci and step responses clearly indicate, location 6 is the most desirable for closed-loop control. For location 1 and 2, the interaction between the controller zero and the first pole prohibitively slowed the system response. Similarly, location 3 and 4 caused the system to behave irregularly under the step input, instead of moving like a first order system. Location 5 was closer to the expected response and location 6 allowed a controller response within the correct timeframe and characteristic response. As the zero value moved farther and farther away, the response to a step input had a lower and lower settling time. In order to be comparable to the proportional controller, values around location 6 and beyond were preferable for comparison's sake. Several zero values were compared to the proportional response in the following figure,

Figure 3.15. This figure utilizes controller gain ( $K$ ) as the independent variable and the resulting settling time as the dependent variable.

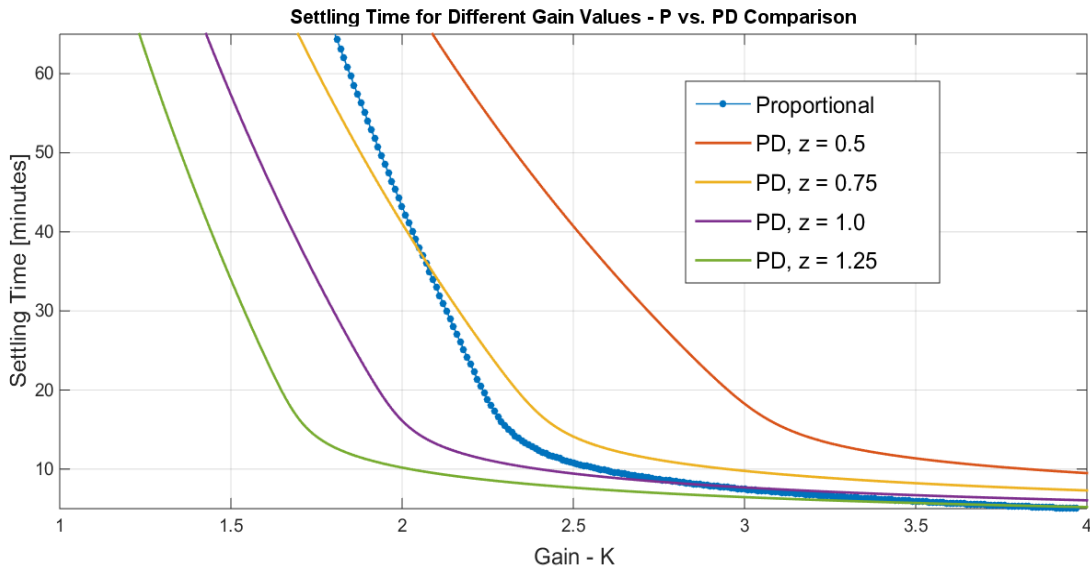


Figure 3.15 – This diagram shows the differences in P and PD Control for a range of gains and a variety of zero values *without saturation*.

The primary metric for choosing a controller gain was settling time. A settling time of 60 minutes was selected for its physical relevance. This is approximately the time that passes from the arrival of professional medical personnel and emergency surgery in the hospital [1]. This timeframe is commonly known as the ‘golden hour’ of medical care. This value also avoided long periods of saturated control, which is physically relevant for the operational life of infusion pumps. A 60 minute settling time was found by combining the results from the above plot with simulation including the saturation value.

From the above analysis, a proportional controller gain of  $K=1.85$  and a proportional derivative zero at  $z=1.25$  with gain  $K=1.27$ , both resulted in the desired settling time of 60 minutes. The final response for the proportional and the proportional derivative controller were

similar both during the transient response and at steady state. The proportional derivative controller allowed a slightly decreased time at the saturation value, but the difference was on the order of about a minute, and negligible. As they are approximately the same, there is no reason to choose a proportional derivative controller over the proportional controller, as it is the simpler of the two and there is no loss of performance during any phase of control.

These analyses were compared with the gains selected by MATLAB's auto tuning feature in SISO Design Tool. This design tool favored proportional control when tested, and even when set to determine a 'PD' compensator, only provided a proportional gain. This gain value of  $K=1.985$  was very similar to the classical gain selection determined in the analysis above for a 60 minute settling time.

### 3.2: Observer-Based State Feedback Control

With classical control operational, the next step was modern control, and the implementation of a state space controller. Each patient transfer function was separated into pole and zero values, shown with the transfer function in Equation 6. These were then placed into the state space representation with the following general equations in observer canonical form:

$$A = \begin{bmatrix} -(P1 + P2) & -P1P2 & 0 \\ 1 & 0 & 0 \\ 0 & 1 & 0 \end{bmatrix} \quad B = \begin{bmatrix} 1 \\ 0 \\ 0 \end{bmatrix} \quad (7)$$

$$C = [K \quad K(Z1 + Z2) \quad K * Z1 * Z2] \quad D = [0]$$

*Where:*

$$\dot{x} = Ax + Bu$$

$$y = Cx + D$$

With this translation, each patient had a characteristic set of matrices in the state space representation. State feedback gains were initially found using pole placement, and then using optimal control (as discussed in the next section). In addition to finding state feedback gains, an observer had to be designed. This is because physically, the only measurable state is blood volume dilution. Therefore, the other two states of the system had to be estimated in order to be useful for control.

The general format used for designing the observer based feedback control is shown in the following figure:

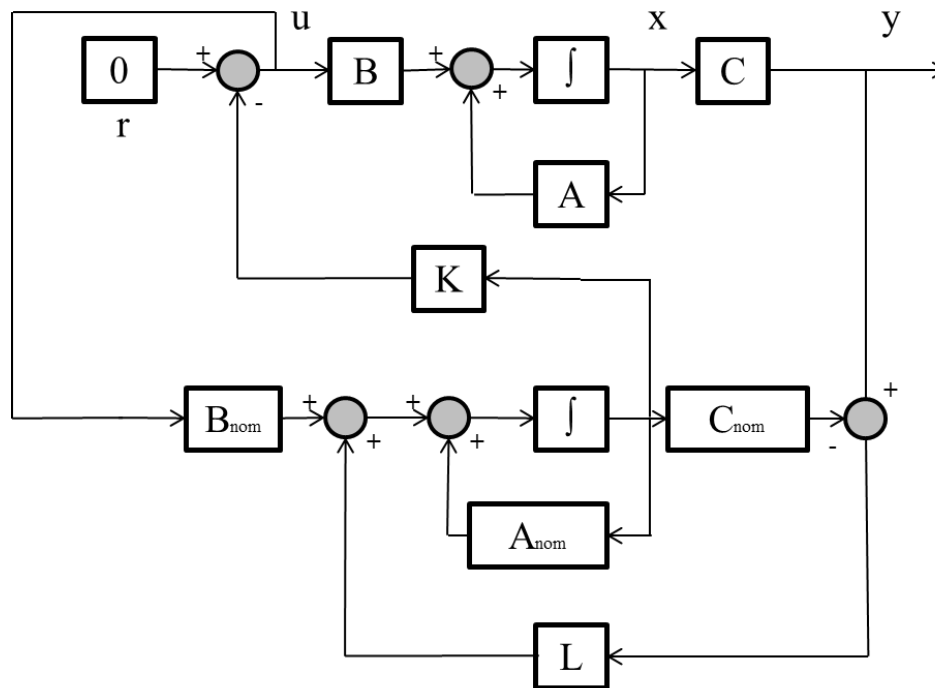


Figure 3.16 – This diagram shows the observer based feedback control implemented in MATLAB, where variables with the subscript ‘nom’, are representative of the nominal patient.

In order to ensure the observer-based feedback control was feasible, the observability and controllability matrices were both calculated. The controllability and observability calculation are shown symbolically below (using the same variables as the state space representation above):

$$[B \mid AB \mid A^2B] = \quad (8)$$

$$\begin{bmatrix} K & K(Z1 + Z2) - K(P1 + P2) & KZ1Z2 - K(P1 + P2)(Z1 + Z2) - K * P1P2 - (P1 + P2)^2 \\ K(Z1 + Z2) & KZ1Z2 - KZ1Z2 & KP1P2(P1 + P2) - KP1P2(Z1 + Z2) \\ KZ1Z2 & 0 & 0 \end{bmatrix}$$

$$[C \mid A'C \mid A'^2C] = \begin{bmatrix} 1 & 0 & 0 \\ -P1 - P2 & 1 & 0 \\ (P1 + P2)^2 - P1P2 & -P1 - P2 & 1 \end{bmatrix} \quad (9)$$

For the nominal case, both the controllability matrix and the observability matrix were of full rank, meaning that the nominal patient is both observable and controllable. In order to see if the simulation in control space was feasible, the controllability calculation had to be performed for all 100 patients. Only the nominal patient was used for the observer, so only one observability matrix needed to be checked. All 100 patients passed the check above for controllability and the nominal patient was observable; thus observer feedback control is possible.

### 3.2.1: Linear Quadratic Regulator Design

Optimal control was determined to be the best way to calculate controller gain values for a physically significant reason: any overshoot in the controller could lead to a patient receiving too much fluid infusion. This made minimizing percent overshoot a priority for the state space controller.

The general equation for the LQR calculation is:

$$J = \int_0^{\infty} [x^T Q x + u^T R u + 2x^T N u] dt \quad (10)$$

The weighting matrices were determined through simulation, and tuned to result in an optimized settling time of 60 minutes. This resulted in the following matrices, which were used within the cost minimization function:

$$Q = \begin{bmatrix} 0.5 & 0 & 0 \\ 0 & 0 & 0 \\ 0 & 0 & 0 \end{bmatrix} \quad (11)$$

$$R = 5$$

As optimal control theory would dictate, the system response was nearly critically damped, and it prevented large overshoot when used in Guyton's model, though due to the differences in the 100 plants, some small overshoot did occur in the final simulation.

### 3.2.2: State Observer Design

Physically, the only measurable state is blood volume dilution, which is the first state in the state space model. In order to account for these physical restraints and enable state feedback control, an observer had to be designed to estimate the second and third state. This observer was

designed using the characteristics of the nominal patient. This way, it could be implemented in simulation with the different transfer functions of 100 patients. As discussed in Section 3.2, the nominal patient is mathematically observable, thus creating a standard Luenberger observer only required finding the correct observer gains. The Luenberger equations are as follows:

$$\begin{aligned}\hat{x} &= A\hat{x} + L[y - \hat{y}] + Bu & (11) \\ \hat{y} &= C\hat{x} + Du\end{aligned}$$

where A, B, C, and D were taken for the nominal patient model, as seen above in Section 3.2.

The observer gains were determined using simple pole placement separate from the controller. A settling time of ten times faster than the state feedback control ( $T_s = 6$  minutes) was the target value for the observer. This observer was designed using an arbitrary input and then combined with the LQR controller, in accordance with the separation principle.

### 3.3: Results and Discussion

First, the controllers were tested by running the simplified blood volume model with a controller based on the nominal patient, and plants based on each of the 100 patients. This was evaluated for each of the three controllers, and shown to be effective in providing the correct infusion for all 100 plant models. Correct infusion is measured by evaluating the blood volume dilution, and having the controller bring it back to a value of zero, which is representative of the state before hemorrhage. The response of the P controller for 100 different plant transfer functions is shown as Figure 3.17. After these results were successfully obtained, the controller was implemented in Guyton's model and the overall blood volume and the blood volume dilution are shown as Figures 3.18 and 3.19, respectively. Then, the difference between the blood

volume at the beginning of the hemorrhage and at the end is calculated and the steady state error is shown below as Figure 3.20.

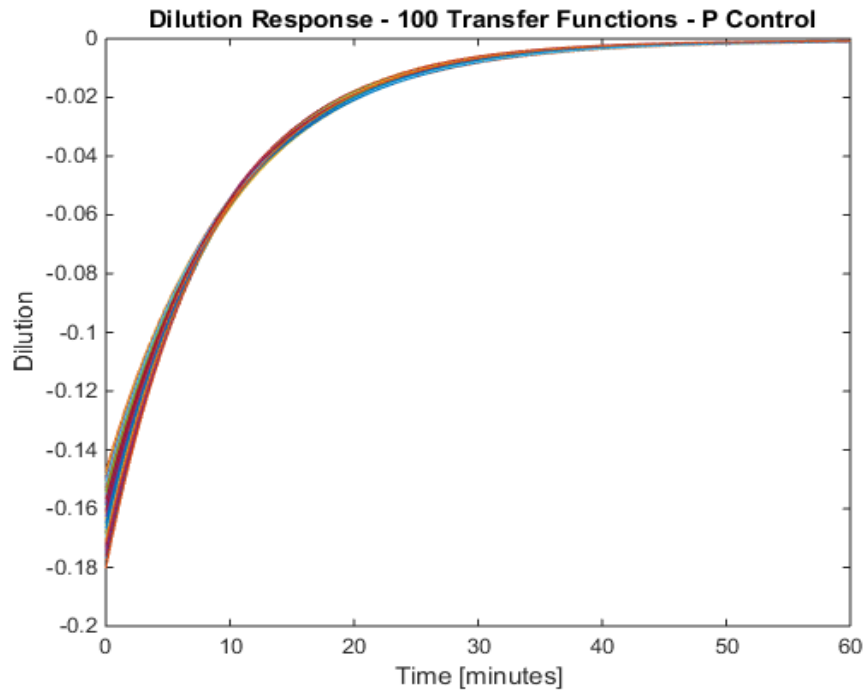


Figure 3.17 – This plot shows that P control takes all 100 transfer functions to the goal value of 100

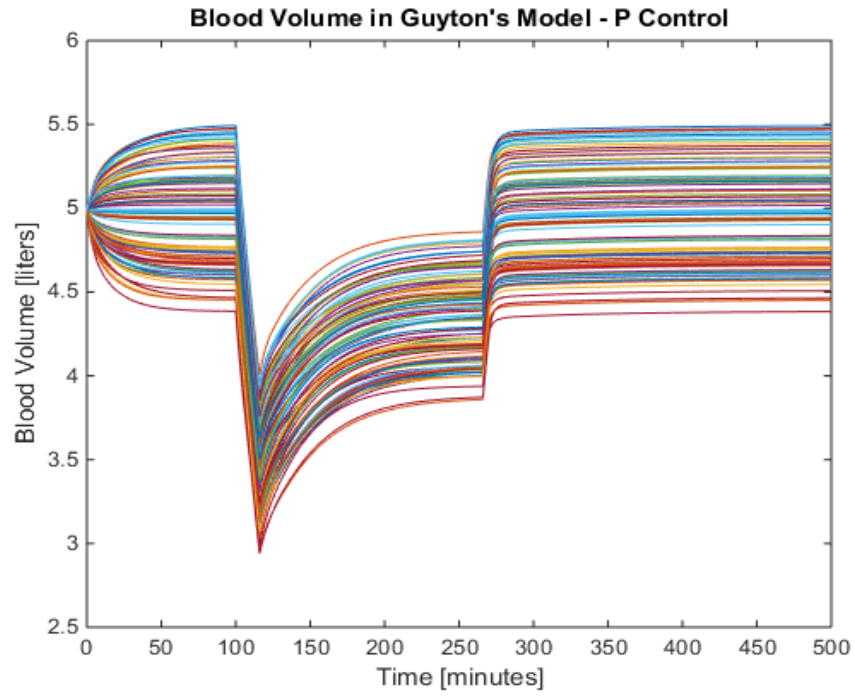


Figure 3.18 – This plot shows the overall blood volume simulated with the  $P$  controller in Guyton's model

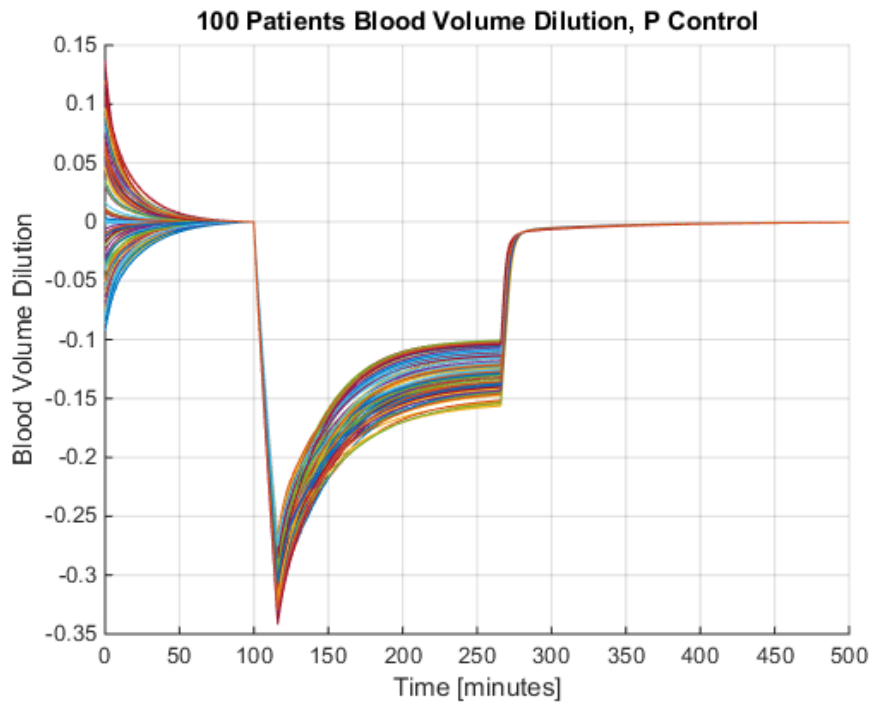


Figure 3.19 – This plot shows the overall blood volume dilution simulated with the P controller in Guyton’s model

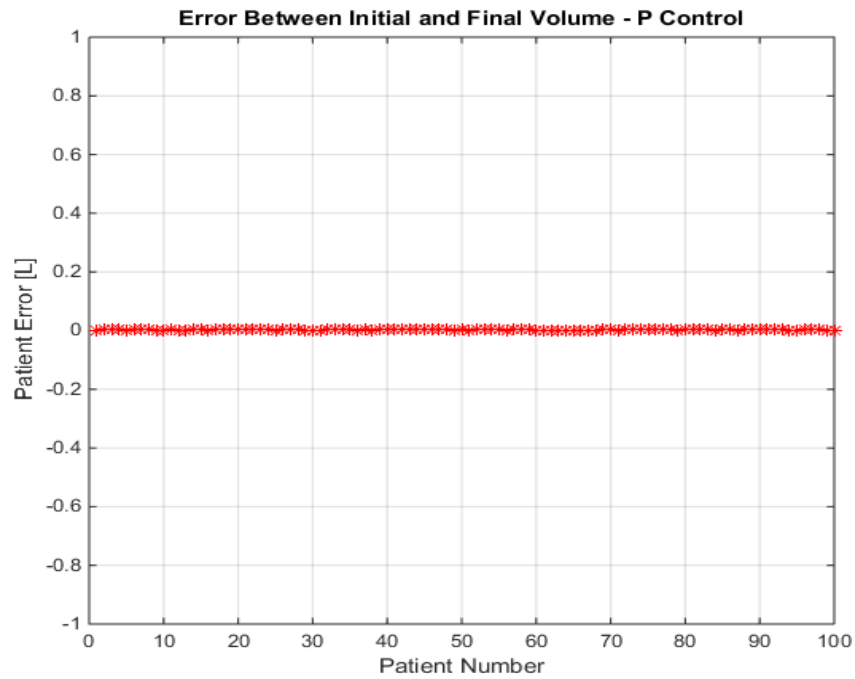


Figure 3.20 – This plot shows the error generated by subtracting the blood volume at the beginning of hemorrhage from the final value for the P Controller

Similarly, these same results are shown for the PD controller in Figures 3.21, 3.22, 3.23, 3.24.

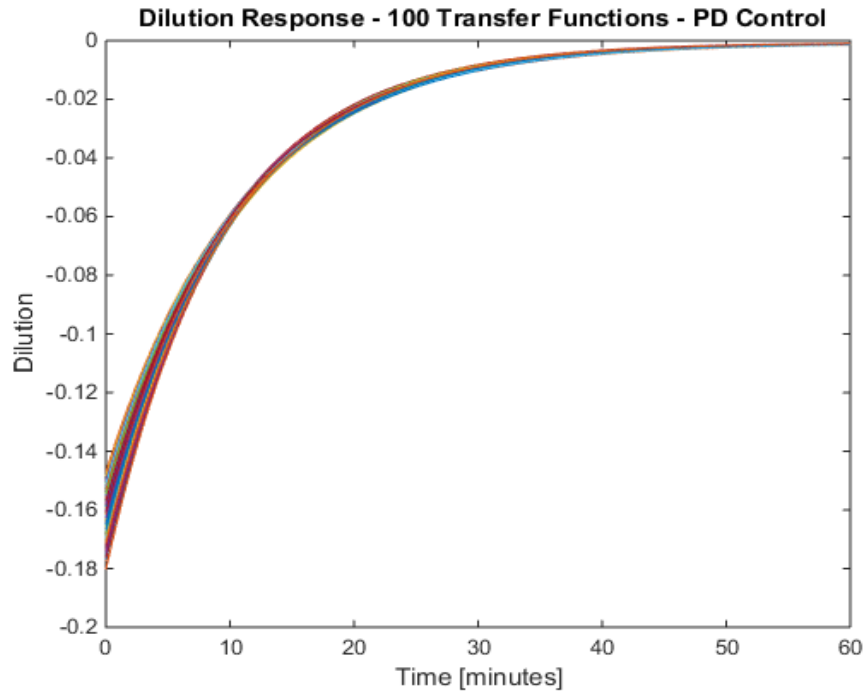


Figure 3.21 – This plot shows that PD control takes all 100 transfer functions to the goal value of 100

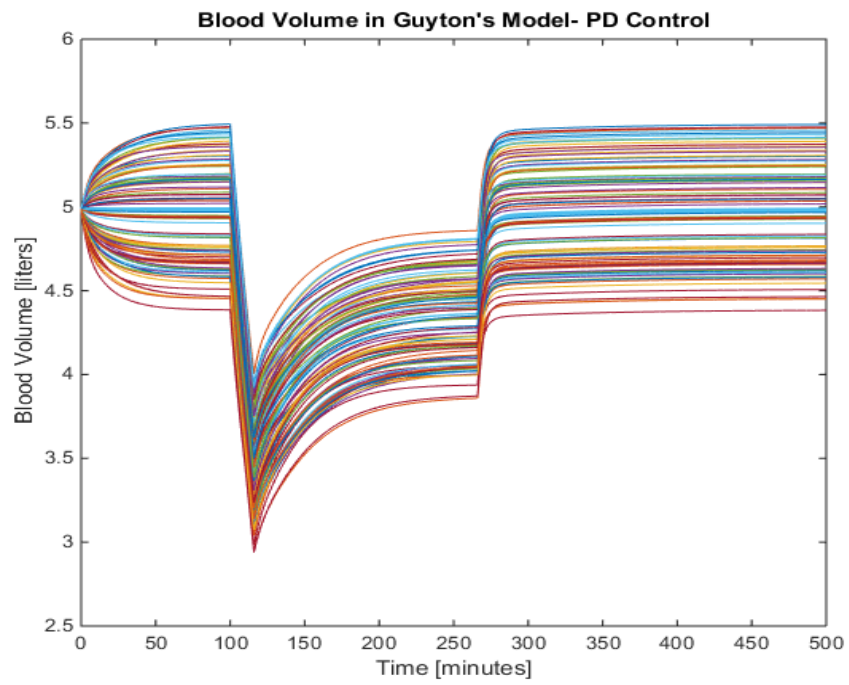


Figure 3.22 – This plot shows the overall blood volume simulated with the PD controller in Guyton's model

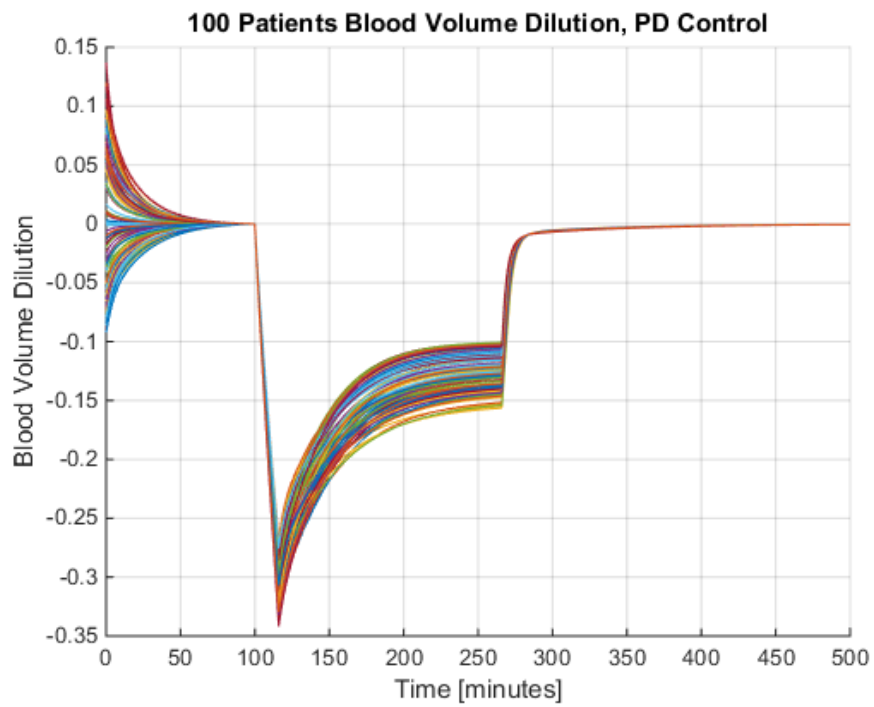
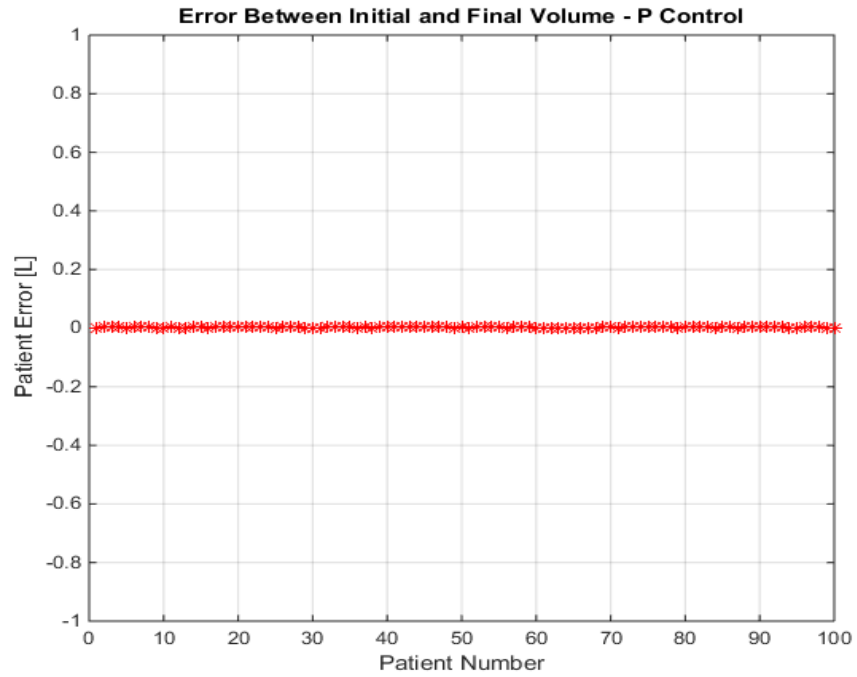


Figure 3.23 – This plot shows the overall blood volume dilution simulated with the PD controller in Guyton's model



*Figure 3.24 – This plot shows the error generated by subtracting the blood volume at the beginning of hemorrhage from the final value for the PD Controller*

Next, these same results are shown for the State Space controller in Figures 3.25, 3.26, 3.27, 3.28.

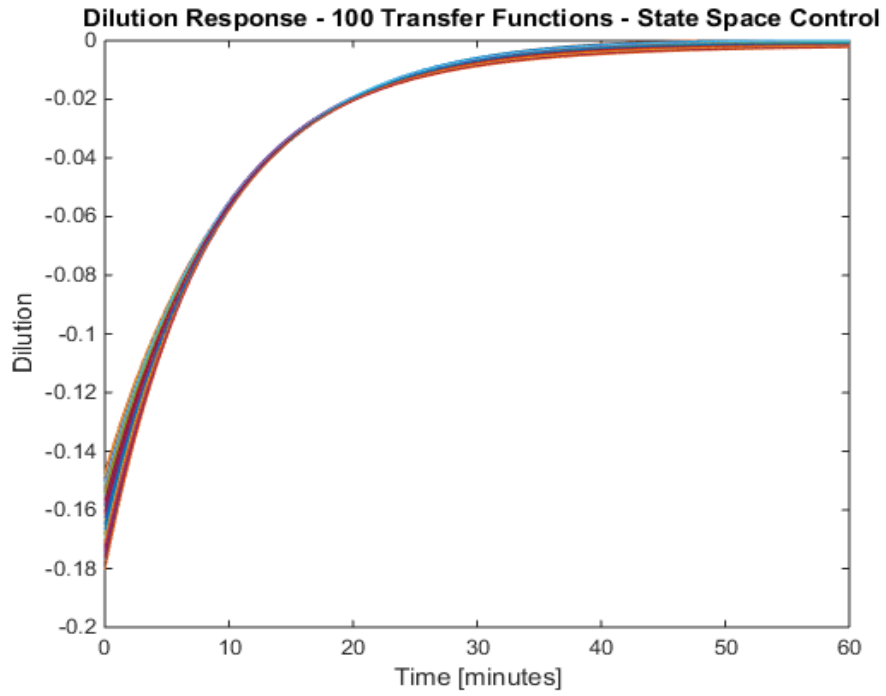


Figure 3.25 – This plot shows that State Space control takes all 100 transfer functions to the goal value of 100

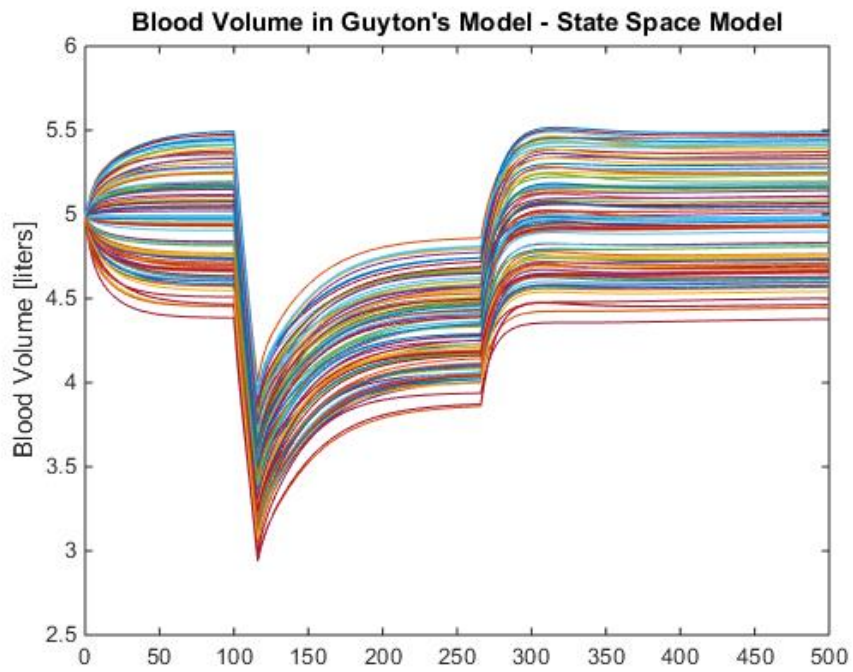


Figure 3.26 – This plot shows the overall blood volume simulated with the State Space controller in Guyton’s model

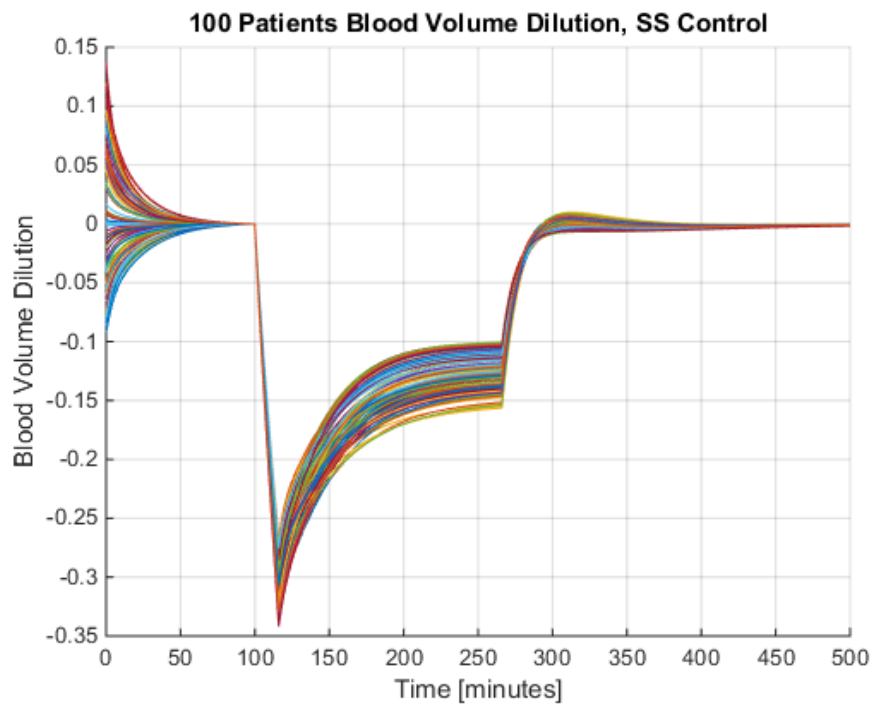


Figure 3.27 – This plot shows the overall blood volume dilution simulated with the State Space controller in Guyton’s model

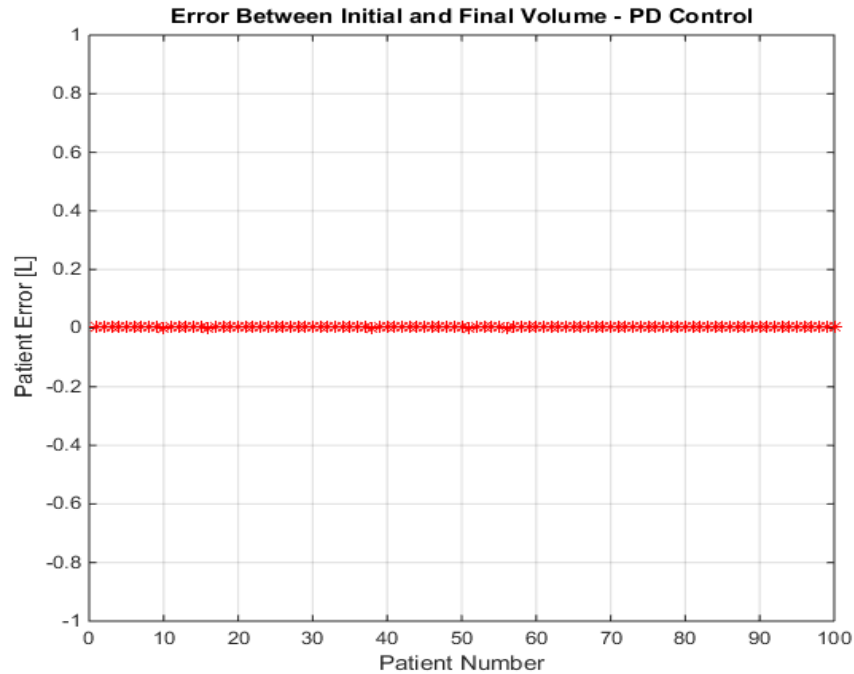


Figure 3.28 – This plot shows the error generated by subtracting the blood volume at the beginning of hemorrhage from the final value for the State Space Controller

As the error plots show, steady state error is very small for all cases. The error produced by the proportional and the proportional derivative controllers were smaller than the state space model. The slight overshoot, as seen in Figure 3.26 allows a little less precision in the long term for the state space model. However, it should be noted that the maximum error of the state space model is still less than 10 mL, which for an infusion of around two liters, is insignificant. It is also important to note that the value of all error points is positive. This is desirable because the error is calculated by subtracting the initial blood volume by the final blood volume. Therefore, all the values of error being positive suggests that over infusion doesn't occur for any patient at steady state.

The nine plots above show the effectiveness of all three controllers in providing infusion to the Guyton model. In actual implementation, the P controller would be the most desirable due to being easily tunable and having a low steady state error.

## Chapter 4: Conclusions and Future Work

### 4.1: Conclusions

A control-oriented model of human blood volume dynamics was validated. Using Guyton's model a data bank of patients was created and used to evaluate a series of closed-loop fluid resuscitation controllers including P, PD and observer-based LQR. All these controllers were successful in taking a variety of patients, and by using the nominal patient as the plant, supplying enough fluid to bring the patient back to its normovolemic state from hemorrhagic state. These results show promise and gives motivation towards more rigorous pre-clinical investigations on the closed-loop fluid resuscitation control system.

### 4.2: Future Work

The next steps for this project include 1) rigorous gain tuning, 2) design of more advanced controllers such as robust and adaptive controllers, and 3) experimental study of closed-loop fluid resuscitation.

First, as with almost all control systems, more tuning could likely improve the patient response, e.g., speed up the settling time and reduce the steady state error. Implementing an integration factor to the control could improve the response time: if classical control is the desired route for the control design, implementation of a PID controller may be a superior choice to effectively handle more complicated fluid intervention scenarios. The closed-loop controllers may also be tested on more diverse patients to bolster their validity and effectiveness.

Second, efforts must be made to examine the use of robust and adaptive control design methods for fluid resuscitation. The controllers designed in this thesis are based on nominal patient model and it may not be effective when subject to a diverse physiologic conditions. The potential advantages and disadvantages associated with the use of more advanced control design methods thus need to be explored.

Third, I could see some degree of hardware implementation being worthwhile. Of course, actual testing is a long way off, but it would be interesting to experiment with controlling an actual infusion pump, and analyzing the results.

## BIBLIOGRAPHY

- [1] W.H. Bickell, M. J. Wall Jr., P.E. Pepe, R. Martin, V.F. Ginger, M.K. Allen, and K. L. Mattox. Immediate Versus Delayed Fluid Resuscitation for Hypotensive Patients with Penetrating Torso Injuries. In, THE NEW ENGLAND JOURNAL OF MEDICINE 311:1105-1109, October 27, 1994.
- [2] F. Javed, A. V. Savkin, G.S.H. Chan, J.D. Mackie, and N.H. Lovell. Identification and Control for Automated Regulation of Hemodynamic Variables During Hemodialysis. In, IEEE TRANSACTIONS ON BIOMEDICAL ENGINEERING, VOL. 58, NO. 6, JUNE 2011.
- [3] A. Cervera and G.Moss. Crystalloid Distribution Following Hemorrhage and Hemodilution: Mathematical Model and Prediction of Optimum Volumes for Equilibration at Normovolemia. In, THE JOURNAL OF TRAUMA, VOL. 14, NO. 6, 1974.
- [4] H. Champion, L. Sturdivan, J. Nolan, M. Stega, R. A. Cowley, W. Sacco, and W. Gill. A Mathematical Model for Volume Replacement in Bleeding Patients. In, JOURNAL OF SURGICAL RESEARCH 19, pp. 297-302. 1975.
- [5] F. Lewis. Prehospital Intravenous Fluid Therapy: Physiologic Computer Modelling. In, THE JOURNAL OF TRAUMA, VOL. 26, NO. 9. 1986.
- [6] R. L. Wears and C. N. Winton. Load and Go Versus Stay and Play: Analysis of Prehospital IV Fluid Therapy by Computer Simulation. In, ANNALS OF EMERGENCY MEDICINE. 2 FEBRUARY 1990.
- [7] S. N. Mardel, S. H. Simpson, S. Kelly, R. Wytch, T.F. Beattie, and G. Menezes. Validation of Computer Model of Haemorrhage and Transcapillary Refill. In, MEDICAL ENGINEERING & PHYSICS, VOL. 17, NO. 3, pp. 215-218. 1995.
- [8] S. H. Simpson, G. Menezes, S. N. Mardel, S. Kelly, R. White, and T. Beattie. A Computer Model of Major Haemorrhage and Resuscitation. MEDICAL ENGINEERING & PHYSICS, VOL. 18, NO. 4, pp. 339-343. 1996.
- [9] A. Hirshberg, D. B. Hoyt, and K. L. Mattox. Timing of Fluid Resuscitation Shapes the Hemodynamic Response to Uncontrolled Hemorrhage: Analysis Using Dynamic Modeling. In, THE JOURNAL OF TRAUMA, VOL. 60, NO. 6. 2005.

- [10] J. C. Pirkle and D. S. Gann. Restitution of Blood Volume After Hemorrhage: Mathematical Description. AMERICAN JOURNAL OF PHYSIOLOGY, VOL. 228, NO. 3. MARCH 1975.
- [11] A. Hedlund, B. Zaar, T. Groth, and G. Arturson. Computer Simulation of Fluid Resuscitation in Trauma. I. Description of an Extensive Pathophysiological Mode and its First Validation. COMPUTER METHODS AND PROGRAMS IN BIOMEDICINE 27. 1988.
- [12] M. C. Mazzoni, P. Borgström, K. Arfors, and M. Intaglietta. Dynamic Fluid Redistribution in Hyperosmotic Resuscitation of Hypovolemic Hemorrhage. In, THE AMERICAN PHYSIOLOGICAL SOCIETY. 1988.
- [13] O. Barnea and N. Sheffer. A Computer Model for Analysis of Fluid Resuscitation. In, COMPUTERS IN BIOLOGY AND MEDICINE, VOL. 23, NO. 6, pp. 443-454. 1993.
- [14] D. E. Carlson, M. D. Kligman, and D. S. Gann. Impairment of Blood Volume Restitution After Large Hemorrhage: a Mathematical Model. In, THE AMERICAN PHYSIOLOGICAL SOCIETY. 1996.
- [15] C. C. Gyenge, B. D. Bowen, R. K. Reed, and J. L. Bert. Preliminary Model of Fluid and Solute Distribution and Transport During Hemorrhage. ANNALS OF BIOMEDICAL ENGINEERING, VOL. 31, pp. 823-839. 2003.
- [16] C. Svensén and R. G. Hahn. Volume Kinetics of Ringer Solution, Dextran 70, and Hypertonic Saline in Male Volunteers. ANESTHESIOLOGY, VOL. 87, NO. 2. AUG 1997.
- [17] D. Drobin and R. G. Hahn. Kinetics of Isotonic and Hypertonic Plasma Volume Expanders. ANESTHESIOLOGY, VOL. 90, NO. 1. JAN 1999.
- [18] D. Drobin and R. G. Hahn. Volume Kinetics of Ringer's Solution in Hypovolemic Volunteers. ANESTHESIOLOGY, VOL. 96, NO. 6. JUN 2002.
- [19] R. Bighamian, A.T. Resiner, and J. Hahn. A Control-Oriented Model of Blood Volume Response to Hemorrhage and Fluid Resuscitation. In, PROCEEDINGS OF THE ASME 2015 DYNAMIC SYSTEMS AND CONTROL CONFERENCE. DSCC2015-9847, OCTOBER 2015

- [20] A. C. Guyton. CIRCULATORY PHYSIOLOGY III: ARTERIAL PRESSURE AND HYPERTENSION. 1980.
- [21] N. Patel, R. Branson, M. Salter, S. Henkel, R. Seeton, M. Khan, D. Solanki, A. Koutrouvelis, H. Li, A. Indrikovs, and M.P. Kinsky. Intrathoracic Pressure Regulation Augments Stroke Volume and Ventricular Function in Human Hemorrhage. In SHOCK, VOL. 44, pg. 55-62, AUGUST 2015